

Bertil Halle
Vladimir P. Denisov
Physical Chemistry 2,
Lund University,
P. O. Box 124,
S-22100 Lund, Sweden

Received and accepted 1 November 1999

Water and Monovalent Ions in the Minor Groove of B-DNA Oligonucleotides as Seen by NMR

Abstract: During the past 8 years, two complementary nmr techniques—magnetic relaxation dispersion and nuclear Overhauser effect spectroscopy—have been applied extensively to the study of water and monovalent ions in the minor groove of B-DNA oligonucleotides in solution. In this review, the possibilities and limitations of the two methods are outlined, with emphasis on the interpretational steps whereby molecular-level information is extracted from the primary data. The results on sequence-dependent hydration and ion–DNA interactions obtained so far by these methods is summarized and critically assessed. The nmr results are also compared with structural data from x-ray crystallography. © 2000 John Wiley & Sons, Inc. *Biopoly* 48: 210–233, 1998

Keywords: nmr; magnetic relaxation dispersion; nuclear Overhauser effect spectroscopy; B-DNA; minor groove; hydration; ion binding; residence time; review

INTRODUCTION

It has long been appreciated that the conformational stability (A, B, . . . , Z forms) and association equilibria (with proteins and drugs) of the DNA double helix are sensitively attuned to its interactions with water¹ and inorganic ions.² From a biological point of view, the essential property of DNA is its particular sequence of nucleotide bases, rather than its global hydration or its counterion atmosphere. To understand DNA function, it is therefore important to examine how hydration and ionic interactions depend on nucleotide sequence. This has been possible only during the last two decades, when synthetic oligonucleotides have been widely available.

X-ray crystallography has provided a detailed structural view of sequence-dependent DNA hydration.³ The first single-crystal x-ray structure of B-DNA, that of the self-complementary dodecamer duplex [d(CGCGAATTCGCG)]₂, revealed a zigzag chain of ordered water molecules in the central part of

the minor groove (Figure 1).⁴ Hydration patterns similar to this so-called spine motif have been found subsequently in the minor groove of many other B-form oligomers containing stretches of four or more AT base pairs (so-called A-tracts). Recently, structures of hydrated oligonucleotides have been solved to atomic resolution (ca. 1 Å) by a combination of “crystal engineering,” flash cooling, and third-generation synchrotron x-ray sources.^{3,5} Whereas a very detailed structural picture of DNA hydration is now emerging, the counterions in oligonucleotide crystals have largely escaped detection. Even at atomic resolution, sodium ions cannot be directly distinguished from water molecules. Even for heavier alkali metals (K⁺, Rb⁺, Cs⁺) and divalent ions (Mg²⁺, Ca²⁺), only a fraction of the counterions have been localized.³

While x-ray crystallography provides unsurpassed structural detail, it does not answer all questions. Most atomic-resolution studies were performed at cryogenic temperatures (100–160 K), where the thermal energy is a factor 2–3 smaller than at room tempera-

Correspondence to: B. Halle; email: bertil.halle@fkem2.lth.se
Biopolymers (Nucleic Acid Sciences), Vol. 48, 210–233 (1998)
© 2000 John Wiley & Sons, Inc.

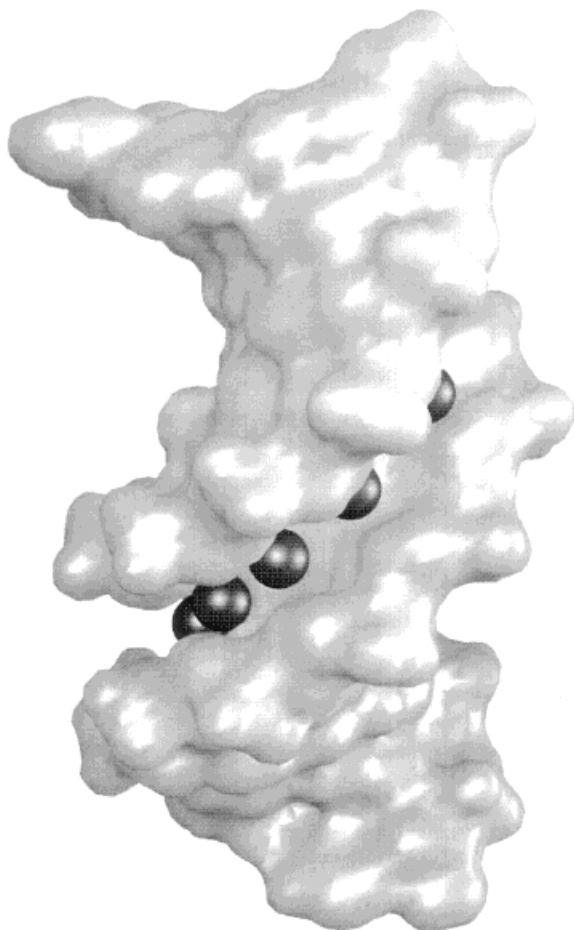


FIGURE 1 Water molecules at the floor of the minor groove in the central A-tract of the [d(CGCGAAT-TCGCG)]₂ duplex. The dark spheres represent the oxygen atoms of water molecules. The helix axis is tilted to expose the minor groove. The picture is based on atomic coordinates from a 1.1 Å resolution crystal structure at 120 K (NDB code BD0007).⁵

ture. At these low temperatures, structure and thermodynamics tend to be dominated by enthalpic effects (interactions), whereas at room temperature, enthalpy-entropy compensation is a recurrent theme.^{6,7} The low water content and crystal packing effects are also of potential concern, particularly for long-range ionic interactions. Finally, conventional crystallography provides no direct information about dynamics. Water molecules and counterions in the minor groove exchange with the surrounding solvent medium. The rates of such exchange processes have no direct bearing on thermodynamic properties (such as conformational stability and association equilibria), but they do relate to conformational dynamics and binding mechanisms. Information about exchange kinetics can therefore be important for understanding DNA function.

To explore fully the roles of sequence-dependent hydration and ionic interactions in DNA function, crystallography must be complemented by techniques that can probe dynamics under physiologically relevant solution conditions. Among the techniques that meet these demands, nmr is arguably the most informative. Nuclear magnetic resonance studies of DNA hydration⁸ and of DNA-ion interactions⁹ have a long history, but it is only in the last few years that the methodology has been developed to a stage where sequence-dependent hydration and ion binding can be studied in molecular detail. Two different nmr methods are currently used for this purpose—one of them records the magnetic relaxation dispersion (MRD) of the water (²H and ¹⁷O)¹⁰ or counterion (e.g., ²³Na)¹¹ resonance, and the other measures the intermolecular nuclear Overhauser effect (NOE) between water¹² or counterion (e.g., NH₄⁺)¹³ protons and specific DNA protons. Since they probe different aspects of the water-DNA or ion-DNA interaction and have different ranges of applicability, the MRD and NOE methods are highly complementary.

The aim of the present review is to summarize and assess critically the information obtained by the MRD and NOE methods about sequence-dependent DNA hydration and ion-DNA interactions in aqueous solution. We discuss only B-DNA (and its complexes with drugs), omitting from consideration the relatively few nmr studies of other DNA conformations, RNA, and protein-DNA complexes. The review is further restricted to water and monovalent ions in the minor groove, which has been the focus of the vast majority of MRD and NOE studies. After introducing the methodology, we discuss the results so far provided by the MRD and NOE methods on water and monovalent ions in the minor groove of B-DNA oligonucleotide duplexes. Whenever possible, we examine the consistency between results obtained by the two nmr methods. Throughout the discussion, we relate nmr results to structural data obtained by x-ray crystallography.

NMR METHODOLOGY

As compared to x-ray crystallography, the nmr methods are indirect. Because water and ions in the minor groove exchange rapidly (on the chemical shift time scale) with bulk solvent, only a single averaged water or counterion resonance is observed. The primary information therefore resides not in chemical shifts but in magnetic relaxation rates—either autorelaxation rates (MRD) or cross-relaxation rates (NOE)—that describe the macroscopic evolution of

an ensemble of nuclear spins after an external perturbation. These magnetic relaxation rates would be of little interest per se if they did not contain information about the molecular degrees of freedom. The molecular interpretation of magnetic relaxation rates rests on a rigorous theoretical foundation,¹⁴ but due to the complexity of biomolecular systems, it is not always straightforward. In the following, we discuss the information content of the primary observables in the MRD and NOE methods with a minimum of theoretical sophistication. More technical treatments are available.^{10,12} Our aim here is to bring out the capabilities and limitations of the two methods and to stress their complementarity. We focus on hydration studies, which account for the vast majority of the literature. However, special considerations related to ion-binding studies are included at the end of each subsection.

Magnetic Relaxation Dispersion

In a typical MRD study of DNA hydration, the longitudinal magnetic relaxation rate R_1 of the ^2H or ^{17}O nucleus in the water molecule is measured by a direct pulse experiment. The strength of the applied static magnetic field is then changed and a new R_1 measurement is performed. Because the field strength is proportional to the resonance frequency ν_0 , the result of an MRD study is usually displayed as a (semilogarithmic) plot of R_1 vs ν_0 —the dispersion profile (Figure 2). All water molecules interacting with DNA exchange rapidly (on the chemical shift and relaxation time scales) with water molecules in the bulk of the solution. Every water molecule in the sample therefore contributes to the resonance peak and the measured relaxation rate R_1 is a population-weighted average over water molecules in all local environments. This is referred to as exchange averaging. Under such fast-exchange conditions, both ^2H and ^{17}O relaxation is (effectively) exponential and can therefore be fully characterized by a single relaxation rate R_1 .

For MRD studies of hydration, the ^1H resonance would seem to be the natural choice. The ^1H nucleus not only yields a stronger nmr signal, but also provides access to much higher frequencies than ^2H or ^{17}O . (At a given magnetic field, the resonance frequency of ^1H is roughly a factor 7 higher than for ^2H or ^{17}O .) The most serious drawback of the ^1H isotope is that exchange averaging mixes not only different types of water protons but also labile DNA protons with exchange times shorter than about 100 ms. In the dodecamer $[\text{d}(\text{CGCGAATTCGCG})]_2$, roughly half of the 56 labile protons have exchange times in the range

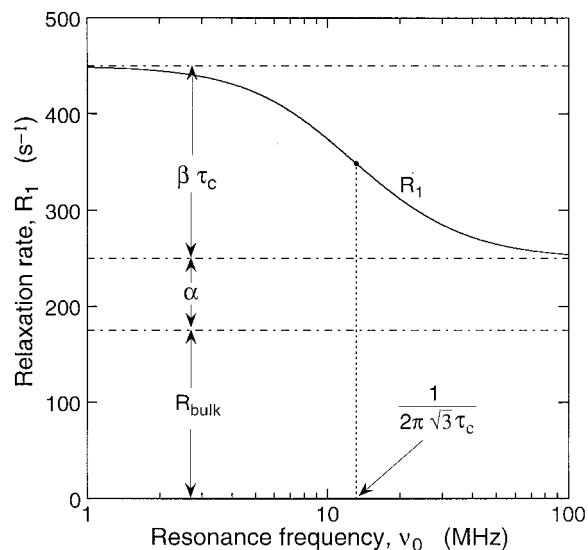


FIGURE 2 Typical water ^{17}O relaxation dispersion profile from a biomolecular solution. The bulk water relaxation rate R_{bulk} is constant throughout the experimentally accessible frequency range. The long-lived water molecules associated with the biomolecule give rise to a dispersion, centered at $\nu_0 = 1/(2\pi\sqrt{3}\tau_c)$. The parameters α and β determine the high-frequency and low-frequency plateaus, respectively, of the dispersion profile.

1–100 ms at 10°C even in the absence of exchange catalysts (such as buffers).¹⁵ Even at 4°C, the water ^1H dispersion is dominated by amino, imino, and (terminal) hydroxyl protons.¹⁵ Since labile deuterons relax 1–2 orders of magnitude faster than the corresponding labile protons, the ^2H relaxation rate is less affected by labile hydrogens. At 4°C and below, the labile-hydrogen contribution to R_1 thus appears to be negligible for ^2H .^{15,16} In doubtful cases, ^{17}O is the isotope of choice, since it reports exclusively on water molecules. The molecular information provided by ^2H and ^{17}O MRD data is to some extent complementary. It can therefore be useful to record both ^2H and ^{17}O dispersion profiles from the same sample. The water is then typically D_2O (or a mixture of H_2O and D_2O), enriched to 10–20% in the ^{17}O isotope for sensitivity reasons (the natural abundance of ^{17}O is merely 0.037%).

The water ^2H or ^{17}O dispersion profile from a DNA solution usually is represented accurately by the theoretical expression¹⁰

$$R_1 = R_{\text{bulk}} + \alpha + \beta[0.2j_Q(\omega_0) + 0.8j_Q(2\omega_0)] \quad (1)$$

where $\omega_0 = 2\pi\nu_0$, R_{bulk} is the (directly measured) relaxation rate in the absence of DNA, and the quadrupolar spectral density $j_Q(\omega)$ is of Lorentzian form:

$$j_Q(\omega) = \tau_C / [1 + (\omega\tau_C)^2] \quad (2)$$

The first step in the analysis of MRD data is to determine, by a nonlinear fit, the three parameters α , β , and τ_C in Eqs. (1) and (2). The phenomenological significance of these parameters is indicated in Figure 2— α defines the excess (above R_{bulk}) relaxation rate on the high-frequency plateau above the dispersion, τ_C is inversely related to the midpoint frequency of the dispersion, and $\beta\tau_C$ is the magnitude of the dispersion step. To accurately determine all three parameters, R_1 must be measured over nearly two decades. If τ_C is in the nanosecond range, this can be done with a field-variable electromagnet (1–10 MHz) and a series of fixed-field superconducting magnets (10–100 MHz).

The microscopic significance of the dispersion parameters obtained from a water ^2H or ^{17}O MRD study of an aqueous oligonucleotide solution is as follows. The β term in Eq. (1) is the contribution from a small number N_β of water molecules with relatively long residence time τ_W . To date, such long-lived water molecules have only been found in the minor groove. The amplitude parameter β is given by

$$\beta = (N_\beta/N_T)\omega_Q^2 S^2 \quad (3)$$

where N_T is the (known) total number of water molecules per DNA duplex in the solution, ω_Q is the rigid-lattice nuclear quadrupole frequency ($8.7 \times 10^5 \text{ rad s}^{-1}$ for ^2H and $7.6 \times 10^6 \text{ rad s}^{-1}$ for ^{17}O), and S is the generalized (intramolecular) orientational order parameter (which may differ for ^2H and ^{17}O). For a fully ordered water molecule, $S = 1$. Fast (compared to τ_W) local motion of long-lived water molecules is manifested primarily as a reduction of the dispersion step (β parameter) via a reduced order parameter $S < 1$.

The α parameter represents the relaxation enhancement of short-lived ($\tau_W \ll \tau_C$) water molecules in direct contact with the DNA surface (ca. 300 for a dodecamer duplex). Some of these are located in the minor groove, but their contribution cannot normally be separated since they are vastly outnumbered by other hydration waters. The magnitude of α typically corresponds to a slowing down of the rotational motion of water molecules in contact with the DNA surface by a factor 6 compared to bulk water.^{15,16} It is important to realize that this is an average over all short-lived hydration waters and that a relatively small fraction of these can make a disproportionately large contribution to the average. Strictly speaking, the separation of the relaxation rate into α and β

contributions is phenomenological—the dispersion of the α contribution simply occurs above the highest accessible frequency. The α/β separation can be given an unambiguous microscopic interpretation only if the identity of the long-lived water molecules is established, e.g., through a difference-MRD experiment (see below).

The correlation time τ_C defines the time scale on which the orientation of long-lived water molecules (in the minor groove) is randomized. This can occur by either (or both) of two independent processes—by rotational diffusion of the entire DNA duplex with rotational correlation time τ_R , or by exchange of long-lived water molecules with bulk water at a rate $1/\tau_W$. These competing processes determine τ_C according to

$$1/\tau_C = 1/\tau_R + 1/\tau_W \quad (4)$$

The rotational diffusion of a B-DNA N -mer duplex is well described by hydrodynamic theory, modeling the duplex as a rigid cylinder of radius 10 Å and length $N \times 3.4$ Å.¹⁷ For a dodecamer in D_2O , τ_R ranges from 5 ns at 25°C to 40 ns at –20°C. These values apply to infinite dilution—at the high DNA concentrations (up to 8 mM duplex) used for MRD work, interactions between nearby DNA molecules may well increase τ_R by a factor 2. For the oligonucleotides so far investigated by MRD, τ_R is much longer than the residence time τ_W of the most long-lived water molecules (in the minor groove of A-tracts). To a good approximation, the residence time can then be obtained directly from the dispersion profile, that is, $\tau_W = \tau_C$. (This also relieves us of the potential complication of anisotropic rotational diffusion of the DNA duplex.) When $\tau_R \gg \tau_W$, the residence time not only governs the position of the dispersion on the frequency axis, but also scales (linearly) the magnitude of the dispersion step (Figure 3). Since the experimentally accessible ^{17}O resonance frequency window currently is about 2–100 MHz, correlation times in the range 1–50 ns can be determined directly from the dispersion profile by ^{17}O MRD. Using the field-cycling technique (applicable to the ^1H and ^2H isotopes), much longer correlation times can be determined.¹⁰ Residence times as long as milliseconds can be determined, also by ^{17}O MRD, from the reduction of the dispersion amplitude when the residence time approaches the spin relaxation time of the bound species.¹⁰

Every water molecule that visits a particular hydration site does not stay there for the same length of time. In fact, the assumption that water exchange can be described as a first-order kinetic process implies a Poisson distribution of residence times (where zero

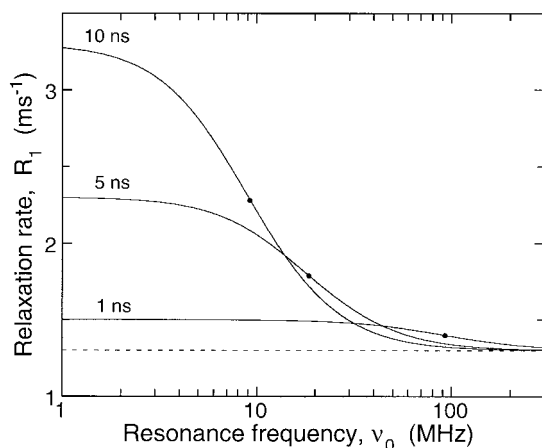


FIGURE 3 Variation of the dispersion profile with the correlation time τ_C . Both the center of the dispersion (marked with a dot) and the magnitude of the dispersion step are affected. The R_1 scale is representative of water ^{17}O relaxation in 8 mM dodecamer solution. ^2H and ^{17}O frequencies above 100 MHz are beyond the reach of present-day nmr magnets.

residence time is most probable). When $\tau_R \gg \tau_W$, the dispersion profile is essentially the Fourier transform of this distribution. The quantity τ_W is actually the mean of the residence time distribution, although it is usually referred to simply as the residence time. (Similar considerations apply to the NOE method.) If the DNA molecule contains several long-lived hydration sites, there is also a distribution of mean residence times τ_W . Such a τ_W distribution has the effect of stretching out the dispersion profile over a wider frequency range. A significant deviation from Lorentzian dispersion shape has not been observed for the oligonucleotides so far examined by MRD.

Although the measured relaxation rate R_1 reflects all water molecules in the sample, the frequency dependence separates the contributions from short-lived (α) and long-lived (β) water molecules (Figure 2). To localize the long-lived water molecules within the structure of the DNA duplex, a difference-MRD experiment must be performed where the dispersion profile is recorded before and after the introduction of a well-defined structural perturbation. For example, long-lived water molecules in the minor-groove of A-tracts can be identified by adding the drug netropsin, which binds with high affinity to this location (Figures 4 and 5).^{15,16} Alternatively, chemically modified nucleotides might be used. The difference-MRD strategy relies, of course, on independent structural information.

The MRD method is not limited to hydration studies, but is applicable to any nucleus that provides

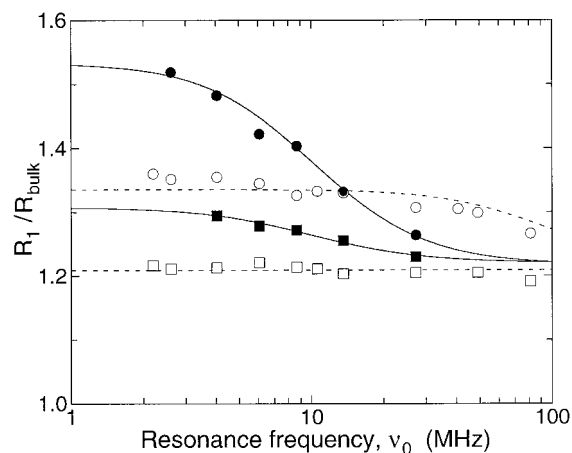


FIGURE 4 Dispersion of the water ^{17}O longitudinal relaxation rate R_1 measured at 4°C (open symbols)¹⁵ and at -20°C (solid symbols)¹⁶ on 8 mM D_2O solutions of the d(CGCGAATTCGCG) duplex at pH 7.0. The dispersion profiles were recorded before (circles) and after (squares) addition of one equivalent of netropsin to the DNA solution. The R_1 data have been normalized by the frequency-independent bulk water relaxation rate R_{bulk} at the respective temperatures. The curves resulted from fits based on Eqs. (1) and (2).

sufficient sensitivity at the required weak magnetic fields. Among the alkali metal ions, ^{23}Na is best suited for MRD studies.^{11,18} While many ^{23}Na relaxation studies of DNA solutions have been reported,¹⁹ only one ^{23}Na MRD study of oligonucleotides has been carried out so far.¹¹ As for ^2H and ^{17}O , the longitudinal relaxation of ^{23}Na is usually effectively exponential, but the transverse ^{23}Na relaxation may be

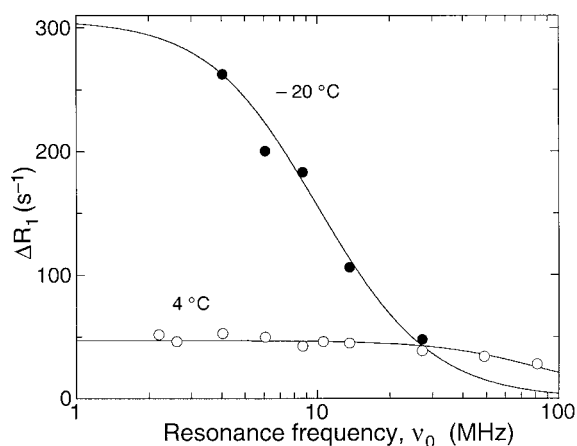


FIGURE 5 The difference induced by netropsin binding in the water ^{17}O longitudinal relaxation rate at 4°C and -20°C. The data points are differences of the R_1 values shown in Figure 4 and the curves were obtained by direct fits to the difference data.

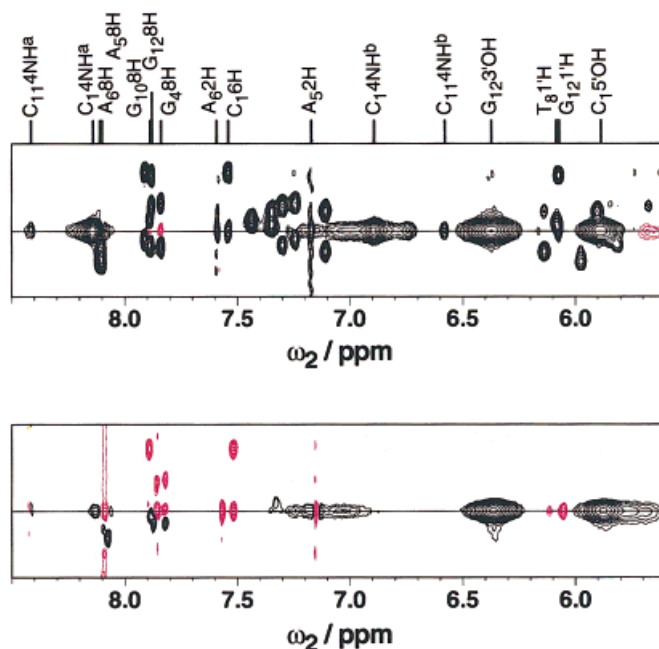


FIGURE 6 Identical regions in ^1H -NOESY (top) and ROESY (bottom) spectra recorded at 10°C from a 4.7 mM aqueous solution (10% D_2O) of the d(CGCGAATTCGCG) duplex at pH 7.0.¹⁵ The mixing time was 60 ms in NOESY and 30 ms in ROESY. The horizontal line indicates the bulk water chemical shift at 4.91 ppm in the indirect (ω_1) dimension. Positive and negative peak amplitudes are shown in black and red, respectively. Resonance assignments are indicated at the top.

significantly biexponential at higher frequencies. (In hydration studies, the transverse relaxation rate R_2 is rarely measured.) There are therefore three relaxation observables, from which the individual spectral densities $j_Q(0)$, $j_Q(\omega_0)$, and $j_Q(2\omega_0)$ can be determined at each field (or ω_0 value) without invoking a motional model. In general, the interpretation of these spectral densities is more complicated than in the case of water ^2H or ^{17}O MRD, because of the intermolecular origin of the quadrupole coupling for monatomic ions. For long-lived ions residing in the minor groove, however, the Lorentzian spectral density in Eq. (2) can still be used and the residence time τ_w can be obtained from Eq. (4). Furthermore, if the coordination geometry is known (from the crystal structure), the quadrupole frequency ω_Q can be estimated from ^{23}Na nmr studies of model compounds.¹¹ The number N_β of long-lived sodium ions (or the ion occupancy in a given site) can then be obtained from Eq. (3).

NOE Spectroscopy

DNA hydration can also be studied by nmr via the relaxation-induced magnetization transfer between dipole-coupled DNA and water protons. This intermolecular magnetization transfer—known as the nuclear

Overhauser effect (NOE)—is formally described by a cross-relaxation rate R_C . Many pulse sequences have been devised to optimize performance and minimize artifacts in NOE hydration experiments.^{12,20} In the most popular version of the NOE experiment, cross relaxation is manifested as a cross peak in a two-dimensional [^1H - ^1H] NOE spectroscopy (NOESY) or rotating frame NOESY (ROESY) spectrum (Figure 6).¹² Because of exchange averaging, there is only a single water resonance in the spectrum (as in the case of MRD) with a chemical shift indistinguishable from that of bulk water. If the DNA ^1H spectrum has been assigned, cross peaks with water can be linked to particular DNA protons. If also the three-dimensional structure of the DNA duplex has been determined (not necessarily by nmr), then the cross peaks can be attributed to the presence of water molecules in spatial proximity (within about 4 Å) of particular proton sites in the DNA molecule. This ability to spatially localize hydration sites is the major strength of the NOE method. (In the MRD method, spatial information can only be obtained by difference experiments.)

Cross peaks at the chemical shift of bulk water can be produced by several mechanisms, as illustrated for an AT base pair in Figure 7. The cross peaks that usually provide information about minor groove hy-

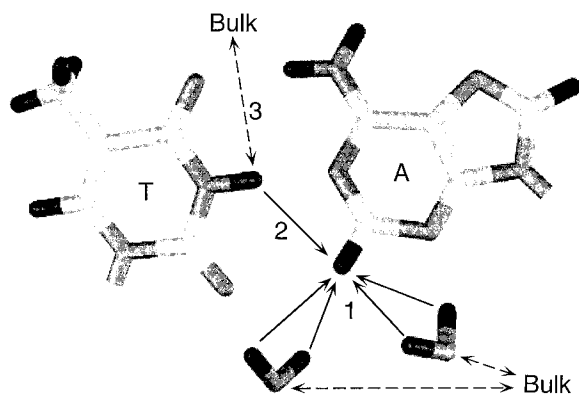


FIGURE 7 Pathways of magnetization transfer between bulk water protons and an adenine H2 proton in the minor groove. The atomic coordinates of the AT base pair and two water molecules at the floor of the minor groove are taken from the same crystal structure as Figure 1. Solid arrows represent magnetization transfer by dipolar cross-relaxation (NOE), while dashed arrows denote magnetization transfer by material exchange of water molecules or protons.

dration are due to magnetization transfer from bulk water to adenine H2 protons. The adenine H2 proton is located at the floor of the minor groove, and if it belongs to an A-tract, has four water protons within 4 Å. The magnetization transfer occurs in two steps. First, the water molecule diffuses from the bulk of the solution into one of the two hydration sites near the adenine H2 proton (dashed arrows). This material transfer of magnetization is followed by NOE transfer (cross relaxation) from the water protons to the nearby adenine H2 proton (solid arrows 1).

A cross peak between water and adenine H2 also can be produced by another mechanism. In the first step of this mechanism (in our example), a water molecule exchanges one of its protons with the labile thymine H3 imino proton (dashed arrow 3). (This step would normally be catalyzed by a hydroxide ion that approaches the imino proton during a base-pair opening event.) In the second step, a NOE transfer occurs from the imino proton to the adenine H2 proton (solid arrow 2). In either of these mechanisms, magnetization transfer must occur during the mixing time τ_M of the NOE experiment (typically, 50–200 ms). Most of the NOE experiments that have been used to study DNA hydration cannot a priori distinguish direct NOEs (pathway 1) from proton-exchange-related NOEs (pathway 2). However, the indirect pathway 2 can be eliminated by saturating the thymine H3 proton during the mixing time (Figure 8).^{20,21} Normally, imino proton exchange is a problem only at or above room temperature, but other labile protons (in particular, the terminal hydroxyl protons) exchange suffi-

ciently rapidly even at lower temperatures and in the absence of exchange catalysts.

A third type of cross peak at the chemical shift of bulk water does not involve any NOE transfer at all, but is entirely due to material exchange of a water proton with a labile DNA proton (dashed arrow 3 in Figure 7). Such pure exchange peaks can be distin-

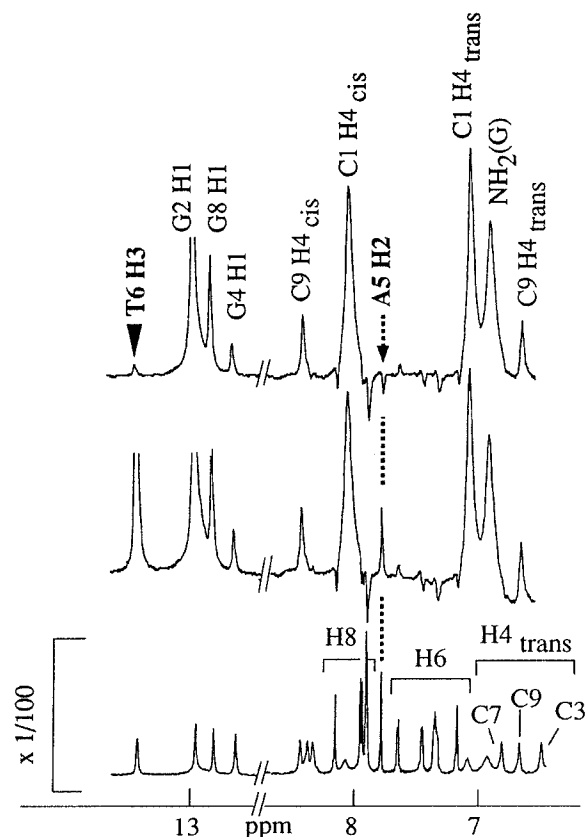


FIGURE 8 The 600 MHz ^1H nmr spectra recorded at 25°C from a 5.5 mM aqueous solution (10% D_2O) of the d(CGCGATCGCG) duplex at pH 7.²⁰ The lower trace is a normal ^1H spectrum for referencing assignments. The middle trace is a one-dimensional NOE spectrum, showing pure exchange peaks with several imino and amino protons and another positive peak at the frequency of the (nonlabile) adenine H2 proton. The upper trace is a one-dimensional NOE spectrum recorded with saturation of the thymine H3 imino proton during the mixing time. The pure exchange peak from this proton is nearly eliminated. Moreover, the adenine H2 peak is now negative, showing that the corresponding positive peak in the middle trace is predominantly due to a proton-exchange-related NOE mechanism. (Reprinted from the *Journal of Molecular Biology* 286, Phan, A. T., Leroy, J. L., Gueron, M., "Determination of the residence time of water molecules hydrating B'-DNA and B-DNA, by one dimensional zero enhancement nuclear Overhauser effect spectroscopy," p. 510, copyright 1999, by permission of the publisher Academic Press.

guished by their positive amplitude in ROESY experiments, where direct and exchange-relayed NOE peaks are negative. However, because pure exchange peaks can be very intense, they may obscure the direct NOE peaks of interest in hydration studies. Thus adenine H2 NOE peaks may overlap with amino proton exchange peaks, while deoxyribose H1' NOE peaks usually overlap with exchange peaks from the terminal hydroxyl protons. Such overlap problems can be largely overcome by so-called NOE-NOESY and ROE-NOESY experiments, where the labile-proton magnetization is back-exchanged to the water during a second mixing period (Figure 9).²²

A fourth type of cross peak at the chemical shift of bulk water is due to a NOE transfer between two (nonlabile) DNA protons, one of which happens to have a chemical shift very close to that of bulk water, for example, a deoxyribose H3' proton. Such degenerate NOEs can be suppressed by a spin-echo filter.²¹ Finally, cross peaks may result from sequential NOEs involving a water proton and several DNA protons, for example, from water to adenine H2 to thymine H3. Such spin-diffusion effects can be diagnosed by varying the mixing time.

If all mechanisms other than a direct NOE between water protons and a DNA proton (such as pathway 1 in Figure 7) can be excluded, then the (integrated) intensity of the cross peak in the NOESY spectrum can be expressed as²³

$$I_{\text{NOESY}} = -(1/2)C_{\text{NOESY}}\text{sgn}(\sigma_{\text{NOE}}) \times [1 - \exp(-R_C\tau_M)]\exp(-R_L\tau_M) \quad (5)$$

where C_{NOESY} is an instrumental scaling factor and $\text{sgn}(x)$ is the signum function. The cross-relaxation rate R_C and the leakage rate R_L are given by

$$R_C = 2|\sigma_{\text{NOE}}| \quad (6a)$$

$$R_L = R_1 + R_1^{\text{ext}} - |\sigma_{\text{NOE}}| \quad (6b)$$

where R_1 is the longitudinal autorelaxation rate of the DNA proton due to its dipole coupling with the water proton and R_1^{ext} is the corresponding rate due to couplings with any other nuclei. In most NOE studies, it is assumed that the mixing time τ_M is much shorter than $1/R_C$ and $1/R_L$, in which case Eq. (5) reduces to

$$I_{\text{NOESY}} = -C_{\text{NOESY}}\sigma_{\text{NOE}}\tau_M \quad (7)$$

This initial-rate approximation is not quantitatively accurate under typical experimental conditions.¹⁵ To

establish the validity of Eq. (7), the dependence of the cross-peak intensity on the mixing time—the NOE build-up curve, $I_{\text{NOESY}}(\tau_M)$ —must be investigated.

The cross-peak intensity I_{NOESY} can provide information about the residence time τ_W of hydration waters via the laboratory-frame dipolar cross-relaxation rate,

$$\sigma_{\text{NOE}} = \omega_D^2 [6j_D(2\omega_0) - j_D(0)] \quad (8)$$

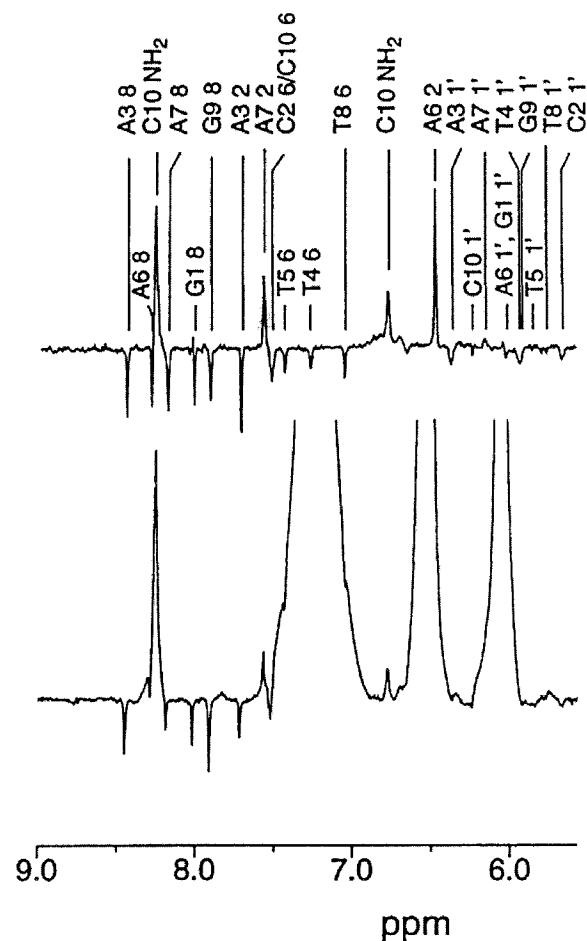


FIGURE 9 Cross-sections through ^1H -NOESY (bottom) and NOE-NOESY (top) spectra recorded at 4°C from a 1.2 mM aqueous solution (10% D_2O) of the d(GCATTAATGC) duplex at pH 7.0.²² The lower trace is the cross-section at the water frequency of a two-dimensional 2D NOESY spectrum (corresponding to the horizontal line in Figure 6) with a mixing time of 50 ms. The upper trace is the cross-section through the diagonal of a 2D NOE-NOESY spectrum with mixing times of 100 and 200 ms. Note that the intense exchange cross peaks in the NOESY spectrum from terminal hydroxyl (at 6.0 and 6.5 ppm) and amino (7.3 and 8.2 ppm) protons are essentially eliminated in the NOE-NOESY spectrum. (Reprinted from Nucleic Acids Research, 24, 2914, 1996, "Minor groove hydration. . .", by permission of Oxford University Press.)

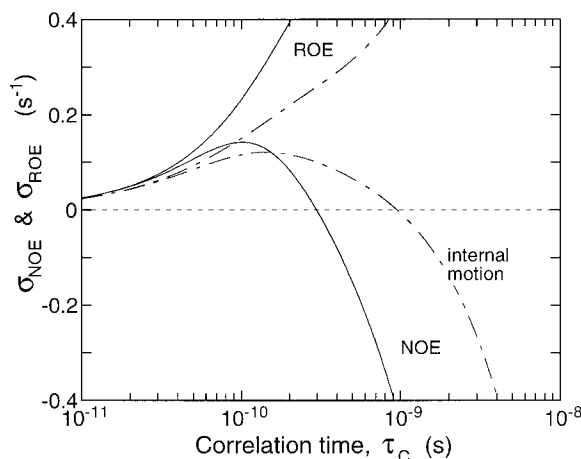


FIGURE 10 Laboratory-frame (σ_{NOE}) and rotating-frame (σ_{ROE}) cross-relaxation rates vs the correlation time τ_C at a resonance frequency $\nu_0 = 600$ MHz. The solid curves refer to the rigid-binding limit, with the rates given by Eqs. (8) and (10) and a Lorentzian spectral density as in Eq. (2). The dashed curves show the effect of internal (water) motion with an order parameter $S = 0.5$ and an internal correlation time of 100 ps. This shifts the zero crossing by a factor 5 toward longer τ_C . In both cases, the cross-relaxation rates were calculated with an effective internuclear separation $r_{\text{eff}} = 2.2$ Å, corresponding to the sum of the dipole couplings of the adenine-6 H2 proton with the four water protons shown in Figure 7.

Here, $\omega_D = 2.4 \times 10^5 (r/\text{Å})^{-3} \text{ rad s}^{-1}$ is the frequency associated with the dipole coupling between a DNA proton and a water proton at separation r . The dipolar spectral density $j_D(\omega)$ is in general a complicated function, reflecting fluctuations in the length and orientation of the internuclear vector due to thermal molecular motions.¹⁴ However, if the water molecule can be considered as rigidly attached to the (rigid) DNA duplex, then the dipolar spectral density $j_D(\omega)$ has the same Lorentzian form [Eq. (2)] as the quadrupolar spectral density $j_Q(\omega)$, with the correlation time τ_C given by Eq. (4). Since the cross-relaxation rate depends strongly on the internuclear separation— $\sigma_{\text{NOE}} \sim 1/r^6$ in the rigid-binding limit—only water protons within about 4 Å of a given DNA proton contribute significantly to the cross peak. In general, several water protons are found within this distance. The total cross-relaxation rate is then given by a sum of terms of the same form as in Eq. (8). If the rigid-binding limit applies and if all water molecules contributing to σ_{NOE} have the same residence time, Eq. (8) can be used directly with an effective two-spin separation $r_{\text{eff}} = (\sum_i r_i^{-6})^{-1/6}$.

In the MRD method, τ_W can be determined directly from the dispersion profile. The extraction of a water residence time from the intensity of a NOESY cross

peak is less straightforward and in most cases only a bound on τ_W can be obtained. This can be done by determining the cross-relaxation rate σ_{NOE} (e.g., from the initial slope of the NOE build-up curve) at several magnetic fields (several ω_0 values) so that ω_D and τ_C can be separated. So far, this approach has not been taken. The usual approach instead exploits the zero crossing of σ_{NOE} (Figure 10). In the rigid-binding limit, the sign of the NOESY cross peak provides a bound on the correlation time for the orientational randomization of the internuclear vector: $\tau_C > \tau_0$ for positive peaks and $\tau_C < \tau_0$ for negative peaks, where $\tau_0 = \sqrt{5}/(4\pi\nu_0)$ is the correlation time at the zero crossing of σ_{NOE} . For the usual ^1H frequencies of 500 and 600 MHz, $\tau_0 = 0.36$ and 0.30 ns, respectively. In the rigid-binding limit, this correlation time may be interpreted according to Eq. (4). Usually, τ_C is much shorter than the duplex tumbling time and can then be identified with the water residence time τ_W . Therefore, one rarely makes a distinction between τ_C and τ_W . (For the dodecamers where τ_W has been quantitatively determined by the MRD or NOE methods, the tumbling correction is at most 10–20%. A larger correction may be needed for shorter oligonucleotides at low temperatures.) In the NOE jargon, water molecules are referred to as “long-lived” or “short-lived” depending on whether their residence times are longer than τ_0 (positive cross peaks) or shorter than τ_0 (negative cross peaks), respectively. In the MRD context, the boundary between the long-lived water molecules that contribute to the β term in Eq. (1) and short-lived ones that are included in the α term is about 1 ns—slightly longer than in the NOE method. When comparing residence times (and bounds) obtained by the NOE and MRD methods, it is important to bear in mind that the (single-field) NOE method yields an effective τ_W that equals the true τ_W only in the rigid-binding limit. If the water molecule(s) undergoes internal motion while it resides in the hydration site, a longer residence time is needed to make σ_{NOE} zero (Figure 10). If the NOE data are analyzed under the assumption of rigid binding, τ_W will therefore be underestimated.

A straightforward method for determining τ_W is to measure the initial rate $dI_{\text{NOESY}}/d\tau_M$, which is proportional to σ_{NOE} [see Eq. (7)], as a function of temperature.²¹ If this rate changes sign within the accessible temperature range, the residence time at the temperature of zero NOE can be identified with τ_0 . Again, this assumes that the rigid-binding limit is applicable. This approach is illustrated in Figure 11. If the temperature dependence of the residence time obeys the Arrhenius law (see subsection on NOE results under Water in the Minor Groove below), so

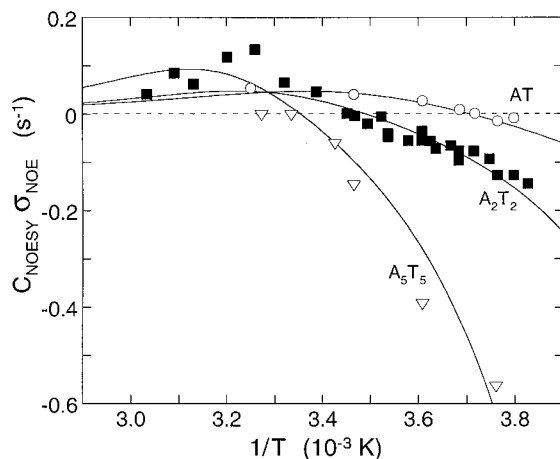


FIGURE 11 Temperature variation of the (negative of the) initial rate of change of the NOESY cross-peak intensity with the mixing time $dI_{\text{NOESY}}/d\tau_M$ for the central adenine H2 proton in three B-DNA duplexes: d(AAAAATTTT) (triangles), d(CGCGAATTCGCG) (squares), and d(CGCGATCGCG) (circles). The rates were measured at 360 MHz.²⁰ The curves were obtained by calculating the cross-relaxation rate σ_{NOE} , as given by Eqs. (2) and (8) with the temperature dependent correlation time taken from the Arrhenius fits in Figure 14, and fitting the proportionality constant C_{NOESY} for each data set.

that $\log(\tau_W)$ scales as $1/T$, then the initial rate curves in Figure 11 should have the same form as the σ_{NOE} curve in Figure 10. This is, indeed, the case.

In principle, τ_W can be determined from σ_{NOE} at any temperature away from the zero crossing, but then one must know the internuclear separations r of all water protons that contribute to the cross peak. Even if such information could be inferred from an atomic-resolution crystal structure, the analysis would be quite sensitive to motional averaging by internal motion (see subsection on NOE results under Water in the Minor Groove below). If NOE experiments are carried out both in the laboratory frame and in the rotating frame, τ_W can be obtained without knowledge of the dipole frequency ω_D .¹² In the rotating-frame NOE experiment (ROESY), the cross-peak intensity in the initial-rate approximation is

$$I_{\text{ROESY}} = -C_{\text{ROESY}}\sigma_{\text{ROE}}\tau_M \quad (9)$$

with the rotating-frame dipolar cross-relaxation rate,

$$\sigma_{\text{ROE}} = \omega_D^2 [2j_D(0) + 3j_D(\omega_0)] \quad (10)$$

Because σ_{ROE} is positive, direct NOE cross peaks are always negative in ROESY spectra. According to Eqs.

(7)–(10), the intensity ratio of corresponding cross peaks in NOESY and ROESY spectra is

$$I_{\text{NOESY}}/I_{\text{ROESY}} = (C_{\text{NOESY}}\tau_M^{\text{NOESY}}/C_{\text{ROESY}}\tau_M^{\text{ROESY}}) \times [6j_D(2\omega_0) - j_D(0)]/[2j_D(0) + 3j_D(\omega_0)] \quad (11)$$

The advantage of using the intensity ratio is that the dependence on the internuclear separation r (via ω_D) cancels out. Provided that all contributing water molecules are in the rigid-binding limit and have the same residence time, Eq. (11) can be used to determine τ_W .^{15,24} Even then, however, the NOESY/ROESY approach has two limitations. First, the instrumental factors C_{NOESY} and C_{ROESY} do not cancel out since the latter includes a resonance offset correction.²⁵ Second, the intensity ratio becomes independent of τ_C when $\omega_0\tau_C \gg 1$. In practice, Eq. (11) can therefore only be used to determine τ_W values near the zero crossing ($\tau_W < 2$ ns at 600 MHz).

Yet another strategy for determining τ_W is provided by the off-resonance ROESY method, where a nonresonant spin-lock field is applied during the mixing period.^{20,26} The cross-relaxation rate determined by this method differs from that in Eq. (10) primarily by the replacement of the spectral density $j_D(0)$ by $j_D(\Omega)$, where the frequency Ω depends on the strength and resonance offset of the radio-frequency field. The main advantage of the off-resonance ROESY method is that a separation of ω_D and τ_C can be achieved (by varying Ω in the neighborhood of $1/\tau_C$) without the need for changing the static magnetic field (which determines ω_0).

The DNA molecule presents only a small number of reporter protons suitable for detecting water molecules. These protons should not exchange within the mixing time and, to avoid contributions from exchange-relayed NOEs, should not have any rapidly exchanging labile proton within about 4 Å. In the minor groove, only the aromatic H2 proton of adenine, the amino N2 protons of guanine, and the deoxyribose H1' protons are sufficiently close to water protons to produce significant cross-peak intensity. The guanine N2 amino protons at the center of the groove floor donate hydrogen bonds to primary hydration waters, but are usually broadened beyond detection by 180° flips of the amino group about the C2—N bond.²⁷ As already mentioned, cross peaks with H1' protons are normally obscured by overlap with intense exchange peaks from terminal hydroxyl protons. Although H1' cross peaks have been observed by means of NOE-NOESY and ROE-NOESY experiments that suppress the exchange peaks,²² the

longer interproton separations render these cross peaks weak even for long-lived water molecules. Furthermore, cross-peak intensities in NOE-NOESY and ROE-NOESY spectra are distorted by relaxation effects and therefore cannot be analyzed quantitatively (except for their sign).²² Therefore, minor groove hydration can essentially be probed only via adenine H2 protons. This means that minor-groove waters residing near GC base pairs usually cannot be detected.

Like the MRD method, the (intermolecular) NOE method is not limited to hydration studies, but can also be used to probe the binding of ions to DNA if the ion contains protons that can engage in NOE transfer. This approach was first used to study binding of ¹⁵N-labeled ammonium ions to a DNA quadruplex²⁸ and has recently been used also with B-DNA duplexes.¹³ In the quadruplex, the bound NH₄⁺ ions exchange slowly on the chemical shift time scale (residence time > 50 ms) and therefore give rise to resonances distinct from the bulk NH₄⁺ resonance.²⁸ In the duplex, however, NH₄⁺ exchange is fast and only a single NH₄⁺ resonance is observed¹³ (as for water).

WATER IN THE MINOR GROOVE

X-ray crystallography has provided a detailed picture of the hydration structure in the minor groove of many B-DNA oligonucleotides.³ The minor groove presents three principal hydrogen-bond acceptors—furanose O4', pyrimidine O2, and purine N3—but only the guanine N2 amino group can donate hydrogen bonds to water. Different types of hydrogen-bond networks anchored at these sites can be established, depending primarily on the groove width. For a groove width of 3–4 Å, as in most A-tracts, only a single file of water molecules can be accommodated. The preferred hydration sites are then at the base steps (between the base-pair planes), where each water molecule forms a strong interstrand hydrogen-bond bridge, e.g., from thymine O2 to adenine N3 in an A-A step. These water molecules cannot form direct hydrogen bonds to each other, but are linked by a second layer of water molecules, as in the spine motif. The narrow-groove morphology characteristic of A-tracts comprising at least four consecutive AT base pairs without an intervening 5'-T-A-3' step is sometimes referred to as the B'-form of DNA.²⁹ For a groove width of about 6 Å, as in the canonical B-form, two ribbons of water molecules can be accommodated at the floor of the minor groove. The hydrogen-bond network is then more variable, with a pref-

erence for intrastrand (often bifurcated) water bridges linking a base O2 or N3 atom with the sugar O4' atom of the adjacent nucleotide in the same strand.

Nuclear magnetic resonance studies of B-DNA hydration have been reported for 21 different oligonucleotides, ranging in length from 7 to 17 base pairs but with a strong overrepresentation of dodecamers (Table I). Among the 12 investigated dodecamers, 8 can be classified as B'-form. Three complexes with minor-groove-binding drugs have also been studied. Of the oligonucleotides listed in Table I, 7 have been studied by MRD and 3 have been studied by both MRD and NOE. Among the NOE studies, all but two^{20,24} are single-field studies (500 or 600 MHz ¹H frequency). With the exception of a single [³H-¹H] NOE study,³⁴ all NOE studies have detected homonuclear [¹H-¹H] magnetization transfer. Most nmr studies of oligonucleotide hydration have been performed below room temperature. At room temperature, the residence time of minor-groove waters is shorter than 1 ns. This is a problem in MRD studies, because the relaxation dispersion then occurs mainly outside (>100 MHz) the accessible frequency windows for ²H and ¹⁷O and the magnitude of the dispersion step is very small. In NOE studies, room-temperature residence times tend to be close to the zero-crossing condition, making NOESY cross peaks hard to detect. A further motivation for using low temperatures in NOE work is to reduce proton exchange rates, thereby attenuating exchange-relayed NOE peaks (that may be mistaken for direct NOE peaks) and pure exchange peaks (that may obscure direct NOE peaks). In MRD work, the reduced hydrogen exchange rates at low temperatures ensure that the labile-hydrogen contribution to the water ²H relaxation rate is negligible. Using emulsion techniques, MRD studies can be carried out at –20°C and below without addition of cryosolvents.¹⁶ To detect the few long-lived minor groove waters against the background of bulk water, MRD studies use high DNA concentrations, typically about 8 mM duplex. Most NOE studies have been carried out at 1–2 mM duplex concentration (Table I).

In this section, we survey the results of the studies listed in Table I. Our aim here is not to be comprehensive—we emphasize what to us appears to be the most significant (and reliable) results. We begin with MRD results. In the discussion of NOE results, we include comparisons with MRD results in an attempt to identify areas of consensus and controversy. Both MRD and NOE results are interpreted and analyzed in the light of the extensive body of structural data provided by x-ray crystallography.

Table I NMR Hydration Studies of B-DNA Oligonucleotides^a

Sequence	<i>N</i> ^b	<i>n</i> (<i>n'</i>) ^c	<i>T</i> (°C)	pH ^d	<i>C</i> ^e (mM)	Method	Ref.
(TGTTTGGC) • (CCAAACA) ^f	7/8	3 (3)	?	7.4	5	NOESY and ROESY (500 MHz)	30
(TGTTTGGC) • (ACAAACA) ^f	7/8	3 (3)	?	7.4	5	NOESY and ROESY (500 MHz)	30
(AAAAATTTT) ₂	10	10 (10)	+4 (−10)–(+35)	6.0 ?	1.0 ?	NOESY and ROESY (600 MHz) Zero-NOE (360, 500, and 600 MHz)	27 20
(CCATTAATGG) ₂	10	6 (3)	+10, 15, 25	5.0–8.6	2.1	NOESY and ROESY (500 MHz)	31
(GCATTAATGC) ₂	10	6 (3)	+4	7.0	1.2	(NOE/ROE)-NOESY (600 MHz)	22
(GCATTAACGC) • (GCGTTAATGC) ^g	10	5 (3)	+4	7.0	2.0	(NOE/ROE)-NOESY (600 MHz)	22
(GCCTTAAAGC) • (GCTTTAAGGC) ^g	10	5 (3)	+4	7.0	1.8	(NOE/ROE)-NOESY (600 MHz)	22
(CGCGATCGCG) ₂	10	2 (2)	(−10)–(+35)	7.0	5.5	Zero-NOE (360, 500, and 600 MHz)	20
(CGAAAATTTTCG) ₂	12	8 (8)	−20	7.0	8.6	¹⁷ O- and ² H-MRD	16
(GCTTTTAAAGC) ₂	12	8 (4)	−20	7.0	8.0	¹⁷ O- and ² H-MRD	16
(CGATATATATCG) ₂	12	8 (2)	−20	7.0	8.4	¹⁷ O- and ² H-MRD	16
(CCTAAATTTGCC) • (GGCAAATTTAGG)	12	7 (6)	+15	6.7	1.1	NOESY and ROESY (500 MHz)	32
(CGCAAATTTGCG) ₂	12	6 (6)	+10 −20	6.0 7.0	1.1 8.2	NOESY and ROESY (500 and 600 MHz) ¹⁷ O- and ² H-MRD	24 16
(CGCAAATTTGCG) ₂ + propamidine	12	6 (6)	+10, 20	6.0	1.1	NOESY and ROESY (500 and 600 MHz)	24
(CGCGAATTCGCG) ₂	12	4 (4)	+5, 10, 25 +4, 10 ? +4, 10, 15, 25 +5, 15 +10 +4 −20 (−15)–(+60)	6.0 7.0 ? 7.0 7.0 7.0 7.0 7.0 7.0 7.0	3 1.2 ? 3.9 8.2 4.7 7.2, 8.0 7.6 3	NOESY and ROESY (600 MHz) NOESY and ROESY (600 MHz) [³ H- ¹ H] HOESY (640 MHz) NOESY (500 MHz) ¹ H-MRD NOESY and ROESY (600 MHz) ¹⁷ O-, ² H-, and ¹ H-MRD ¹⁷ O- and ² H-MRD Zero-NOE (360, 500, and 600 MHz)	33 27 34 35 35 15 15 16 20
(CGCGAATTCGCG) ₂ + propamidine	12	4 (4)	+10	7.0	1	NOESY and ROESY (600 MHz)	36
(CGCGAATTCGCG) ₂ + netropsin	12	4 (4)	+10	7.0	3.3	NOESY and ROESY (600 MHz)	15
(CGCGAAT _{Me} T _{Me} CGCG) ₂ ^h	12	4 (4)	+4 −20 +10, 20	7.0 7.0 7.0	7.2, 8.0 7.6 ?	¹⁷ O-, ² H-, and ¹ H-MRD ¹⁷ O- and ² H-MRD NOESY and ROESY (500 MHz)	15 16 37
(CGCGA _{OH} A _{OH} T _{OH} T _{OH} CGCG) ₂ ⁱ	12	4 (4)	+10, 20	7.0	?	NOESY and ROESY (500 MHz)	37
(GTGGAATTCAC) ₂	12	4 (4)	+4	7.0	1	NOESY and ROESY (600 MHz)	38
(GTGGTTAACAC) ₂	12	4 (2)	+4	7.0	1	NOESY and ROESY (600 MHz)	38
(CTACTGCTTTAG) • (CTAAAGCAGTAG)	12	4 (3)	+5	6.9	2	NOESY and ROESY (500 MHz)	39
(CGCTCTAGAGCG) ₂	12	2 (1)	−20	7.0	7.8	¹⁷ O- and ² H-MRD	16
(TAGCGTACTAGTACGCT) ₂	17	2 (1)	+4 +4	7.0 6.9	3 8.6	(NOE/ROE)-NOESY (600 MHz) ¹⁷ O- and ² H-MRD	40 40

^a Arranged in order of descending values of *N*, *n*, and *n'*.^b *N*: number of base pairs.^c *n*: length of longest sequence of AT base pairs; *n'*: length of longest sequence of AT base pairs without an intervening T-A step.^d Uncorrected for solvent isotope effects.^e Duplex concentration.^f Matched and mismatched duplexes studied with and without a N-(2-hydroxyethyl) phenazinium 5'-tether.^g Singly cross-linked by 3'—(CH₂CH₂O)₆—5' linker.^h T_{Me} = 7'-α-methyl carbocyclic thymidine.ⁱ A_{OH}·T_{OH}: 6'-α-hydroxy carbocyclic adenine and thymidine.

MRD Results

Figure 4 shows water ^{17}O relaxation dispersions from a 8 mM D_2O solution of the d(CGCGAATTCGCG) duplex at 4°C and -20°C, recorded before and after addition of the minor-groove-binding drug netropsin.^{15,16} The observation, in the absence of the drug, of a dispersion demonstrates unambiguously that some of the hydration waters have residence times in the nanosecond range. However, the MRD data do not reveal the location of these long-lived water molecules. Such information can only be obtained by displacing a subset of the hydration waters and recording a new dispersion profile. Netropsin is known to bind tightly to the central A-tract of the minor groove in d(CGCGAATTCGCG). As seen from Figure 4, netropsin binding nearly eliminates the dispersion. From this observation, we can immediately conclude that most of the long-lived waters are among the ones displaced by netropsin, that is, they are located in the minor groove of the central A-tract. The effect of these long-lived water molecules can be displayed more directly by plotting the difference $R_1(\text{free duplex}) - R_1(\text{netropsin complex})$ vs frequency. This difference dispersion is shown in Figure 5 for both temperatures. The beneficial effect of the low temperature is evident. At -20°C, the dispersion is centered in the accessible frequency window and the magnitude of the dispersion step is greatly magnified.

According to Eqs. (1) and (2), the difference dispersion profile is fully determined by the two parameters β and τ_C . (To a good approximation, α cancels out in the difference.) The residence time τ_W is obtained from the correlation time τ_C by means of Eq. (4), where a crude estimate of the duplex tumbling time suffices since $\tau_R \gg \tau_W$. In this way, we obtain $\tau_W = 1.0 \pm 0.2$ ns at 4°C and 11 ± 1 ns at -20°C. With the aid of Eq. (3), the dispersion amplitude parameter β yields $N_\beta S^2 = 5.1 \pm 0.5$ at 4°C and 4.1 ± 0.2 at -20°C. We can thus conclude that netropsin displaces 4–5 fully ordered long-lived water molecules ($S = 1$) or a larger number of partially ordered ($S < 1$) ones. On the basis of molecular volumes, we expect netropsin to displace at least 20 water molecules. Among these, 5 are located at the floor of the groove, where they hydrogen bond to the N3 and O2 atoms of the nucleotide bases.^{3–5} Judging from water residence times in proteins, where more MRD data are available,⁴¹ only these 5 water molecules are expected to have residence times in the nanosecond range, whereas the more exposed water molecules in the outer part of the groove should exchange more rapidly.

If the difference dispersion is attributed to these 5 water molecules, the -20°C β parameter (presumably more accurate than the 4°C value) yields a mean-square order parameter $S^2 = 0.8$, corresponding to libration amplitudes of 10°–15°.¹⁶ Such high orientational order is consistent with the high positional order of these water molecules seen in atomic-resolution crystal structures^{3,5} and may partly reflect local motions of the adjacent nucleotide bases and furanose rings.⁴² Similarly high order parameters are found for the long-lived waters in other dodecamers.¹⁶ It may be estimated that the entropy associated with transfer of these highly ordered water molecules into bulk solvent is comparable to the entropy difference between ice and bulk water.^{16,43} This supports the idea that elimination of ordered water can provide an important entropic driving force for drug binding to the minor groove of DNA.⁶ A quantitative comparison of the ^2H and ^{17}O dispersion amplitudes shows that $N_\beta S^2$ is substantially smaller for ^2H .^{15,16} This indicates that most of the long-lived water molecules are flipping about their dipole axis while residing in the minor groove.¹⁶ These flips of the primary hydration waters may be coupled to the exchange (with bulk water) of the water molecules in the secondary layer, which are hydrogen bonded to the primary waters.

The small dispersion from the netropsin complex corresponds to $N_\beta S^2 = 1.6 \pm 0.4$ and the same residence time as for the 5 displaced waters. Since the groove widens progressively toward the ends of the duplex, this dispersion can reasonably be ascribed to two water molecules residing at the floor of the groove and accepting hydrogen bonds from the amidinium groups at each end of the netropsin molecule. These two water molecules would then have the same order parameter as the 5 displaced water molecules. The value $N_\beta S^2 = 5.9 \pm 0.6$ obtained for the free duplex probably corresponds to 7 long-lived water molecules. The twofold symmetry of the self-complementary duplex (without netropsin) requires N_β to be odd and the experimental $N_\beta S^2$ value implies that $N_\beta > 5$ (since S cannot exceed 1). Although the MRD data do not exclude the possibility that N_β is larger than 7 (say 9 or 11), it is unlikely that water molecules at the wide ends of the groove have the same long residence time as the ones in the narrow A-tract. The observed Lorentzian shape of the dispersion profile indicates that the long-lived water molecules have nearly the same residence time (within a factor 2, say). A wide τ_W distribution would produce a noticeable stretching of the dispersion profile.

^{17}O and ^2H dispersions have been recorded at -20°C for five additional self-complementary dodecamer duplexes with A-tracts of different length and

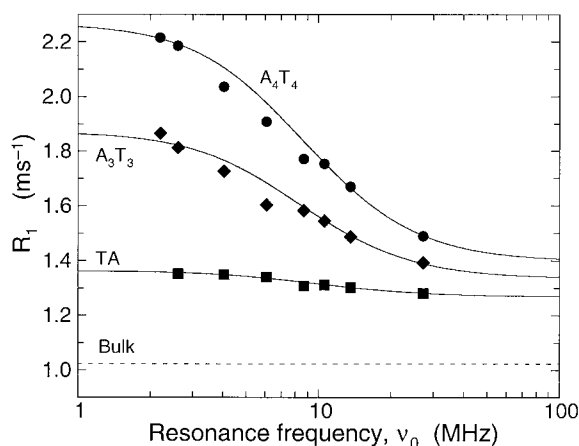


FIGURE 12 Dispersion of the water ^{17}O longitudinal relaxation rate R_1 measured at -20°C on ca. 8 mM HDO solutions of three dodecamer duplexes at pH 7.0: d(CGAAAATTTTCG) (A_4T_4), d(CGCAAATTTGCG) (A_3T_3), and d(CGCTCTAGAGCG) (TA).¹⁶ The curves resulted from fits based on Eqs. (1) and (2). The dashed line represents the relaxation rate R_{bulk} of the pure HDO solvent.

different ordering of the A and T nucleotides¹⁶ (Table I). The magnitude of the dispersion step depends strongly on both base composition and base sequence. The smallest dispersion ($N_\beta S^2 = 1.2 \pm 0.3$) is found for the dodecamer d(CGCTCTAGAGCG) with the shortest A-tract and the largest dispersion ($N_\beta S^2 = 8.6 \pm 0.4$) is found for the dodecamer d(CGAAAATTTTCG) with the longest A-tract (Figure 12). The weak dispersion observed for the d(CGCTCTAGAGCG) dodecamer at -20°C is consistent with the absence of a significant dispersion for the 17-mer d(TAGCGTACTAGTACGCT) at 4°C .⁴⁰ These results indicate that long-lived waters are confined to A-tracts (including the two flanking base steps). Why do water molecules reside longer in A-tracts? Judging from previous MRD results on protein hydration,⁴¹ geometry is the decisive factor. Although an analysis of the crystallographic data base is somewhat confounded by crystal packing effects, it is clear that the minor groove is significantly narrowed in A-tracts (Figure 1). For example, the d(CGCTCTAGAGCG) duplex, which produces the smallest dispersion, has a uniformly wide groove of $6\text{--}7 \text{ \AA}$,⁴⁴ whereas the d(CGCGAATTCGCG)^{4,5} and d(CGCAAATTTGCG)⁴⁵ duplexes have groove widths of $3\text{--}5 \text{ \AA}$ within their A-tracts. The crystal structure of d(CGAAAATTTTCG) has not been reported, but the homo-adenine A-tracts in d(CGCA₆GCG)⁴⁶ and d(CGCGA₆CG)⁴⁷ show minor groove narrowing similar to that in d(CGCGAATTCGCG) throughout their A-tracts.

Although the d(CGCAAATTTGCG) duplex has a 50% longer A-tract than the d(CGCGAATTCGCG) duplex, it produces a slightly smaller dispersion step ($N_\beta S^2 = 5.1 \pm 0.6$ vs 5.9 ± 0.6).¹⁶ This unexpected result can be explained by the crystallographic finding⁴⁵ that the longer A-tract has a slightly wider groove (5.1 vs 4.2 \AA , averaged over the A-tract). Several lines of evidence have suggested that a T-A step within an A-tract widens the groove and disrupts the spine of hydration.^{29,48–50} However, the d(CGATATATATCG) duplex, with three T-A steps, yields a larger dispersion step ($N_\beta S^2 = 7.2 \pm 0.5$) than the d(GCTTTTAAAAGC) duplex, with an A-tract of the same length but with only one T-A step ($N_\beta S^2 = 5.8 \pm 0.7$).¹⁶ The available crystallographic data bearing on this issue are not entirely conclusive.

Overall, the available MRD results are consistent with the crystal structures. Together, these data demonstrate that the number of long-lived water molecules is strongly correlated with the width of the minor groove. Also in proteins, water residence times are largely determined by geometrical factors.⁴¹ Remarkably, the residence time of the long-lived water molecules in the minor groove was found to be essentially the same ($10\text{--}15 \text{ ns}$) for the six dodecamers investigated by MRD at -20°C .¹⁶ Even a single water molecule with a residence time comparable to the duplex tumbling time would have been detected (Figure 3). The near invariance of τ_w among different duplexes, and within the A-tract of a given duplex (see above), suggests that the τ_w distribution for minor-groove water is bimodal. This could be the case if there are two dominant local hydration motifs with either a single or a double file of water molecules at the floor of the groove. Single-file waters (the primary layer of the spine of hydration) have a narrow distribution of long residence times, whereas double-file waters (and all waters in the higher layers of both hydration motifs) have much shorter residence times (and, presumably, a wider distribution). As atomic-resolution crystal structures become available for more oligonucleotides, this conjecture can hopefully be assessed more quantitatively.

NOE Results

Table II lists 15 B-DNA duplexes (including one DNA–drug complex) where direct-NOE cross peaks with adenine H2 protons have been reported. In each case, direct-NOE peaks are assigned in the sequence formula and adenines associated with long-lived (defined here as $\tau_w > 0.5 \text{ ns}$ at 4°C) water molecules are underlined in boldface. With two exceptions, all reported direct-NOE peaks are with adenine H2 pro-

Table II Observed Direct-NOE Peaks with Adenine H2 Protons and Correlation Times Deduced from Peak Intensities

Sequence ^a	τ_c (ns) [T (°C)] ^b					
	Zero-NOE	Ref.	Ratio	Ref.	Intensities	Ref.
CGCG AA TTTCGCG	A ₅ : 0.5 [10], 0.3 [20]	20			A ₅ : > 0.3 [4,10]	15, 27
GCGCT TA AGCGC	A ₆ : 0.5 [15], 0.3 [23]	20	A ₆ : 0.6 [10]	15	A ₆ : > 0.3 [4,10]	27
CGCG AA T _{Me} T _{Me} CGCG					A ₅ ,A ₆ : < 0.4 [10, 20]	37
GCGCT _{Me} T _{Me} AA GCGC						
CGCG AA TTTCGCG		A ₅ : > 0.8 [10]		36		
GCGCT TA AGCGC		A ₆ : > 1.1 [10]		36		
+ propamidine						
CGC AA ATTTGCG		A ₅ : 0.5–1.1 [10]		24	A ₄ : > 0.4 [10]	24
GCGTT TA AAACGC		A ₆ : 0.6–1.5 [10]		24		
CGC AA ATTTGCG		A ₅ : 0.8–2 [10]		24	A ₄ : > 0.4 [10]	24
GCGTT TA AAACGC					A ₆ : > 1.5 [10]	24
+ propamidine						
AAAA TTTTT	A ₃ : 0.5 [20]	20			A ₃ ,A ₄ ,A ₅ : > 0.3 [4]	27
TTTT AAAA	A ₅ : 0.5 [26]	20				
GTGGA AT TCAC					A ₅ ,A ₆ : > 0.3 [4]	38
CACCT TA AGGTG					A ₁₁ : ≈ 0.3 [4]	38
GTGGT TA ACCAC					A ₇ ,A ₈ ,A ₁₁ : ≈ 0.3 [4]	38
CACCA AT TGGTG						
CCT AA ATTTGCC ^c					A ₅ ,A ₆ ,A ₁₆ ,A ₁₇ ,A ₁₈ ,A ₂₂ : > 0.4 [15]	32
GG AT TT TA AAACGG						
CT ACT GCTTTAG ^c					A ₁₅ ,A ₁₆ ,A ₁₇ : > 0.4 [5]	39
GATG AC GA AA ATC					A ₃ ,A ₁₁ ,A ₂₀ ,A ₂₃ : ≈ 0.4 [5]	39
CC AT TA AT TGG					A ₃ : < 0.4 [10,15,25]	31
GGTA AT TACC					A ₆ ,A ₇ : ≈ 0.4 [15]	31
GC AT TA AT TGC					A ₃ : < 0.3 [4]	22
CGTA AT TACG					A ₆ ,A ₇ : > 0.3 [4]	22
GC AT TA AC GC ^c					A ₃ : < 0.3 [4]	22
CGTA AT TGCG					A ₆ ,A ₁₆ : > 0.3 [4]	22
					A ₇ ,A ₁₇ : ≈ 0.3 [4]	22
GCCT TA AAAGC ^c					A ₈ ,A ₁₇ : < 0.3 [4]	22
CGGA AT TTTCG					A ₆ ,A ₇ ,A ₁₆ : ≈ 0.3 [4]	22
CGCG AT TCGCG	A ₅ : 0.5 [–5], 0.3 [10]	20				
GCGCT AG GCGC						
TAGCGT ACTAGTAC GCT					A ₇ ,A ₁₀ ,A ₁₃ : ≈ 0.3 [4]	40
TCGC ATGATCAT GCGAT						

^a Duplex pairing with AT base pairs in boldface. Observed cross peaks with adenine H2 that have been interpreted as direct-NOE peaks are underlined—a bold face line indicates that $\tau_c > 0.5$ ns at 4°C. Cross peaks to adenines that are not underlined were either obscured by overlapping pure exchange peaks, or were considered to be mainly proton-exchange relayed (usually involving the terminal hydroxyls).

^b Correlation time deduced from adenine H2 cross-peak intensity by recording its zero crossing as a function of temperature (first column), by quantitatively analyzing the NOESY/ROESY cross-peak intensity ratio (second column), or by qualitatively observing the NOESY and ROESY cross-peak intensities.

^c Nonsself-complementary sequence.

tons. Very little NOE information is therefore available about hydration of CG base pairs. It should also be noted that the NOE method can provide quantitative information about residence times in the range 0.3–2 ns. For residence times outside this narrow range, only bounds can be obtained.

The “Drew–Dickerson dodecamer” d(CGCGAATTCGCG) has become the benchmark for DNA hydration studies—no less than seven NOE studies of this duplex have been reported (Table I). The four studies that have examined the unmodified duplex all find positive NOESY cross peaks with both adenine H2 protons, that is, with A₅ and A₆ in both strands (Table II). (Because of the twofold symmetry of a self-complementary duplex, the resonances of A₅ and A₁₇ are degenerate, as are A₆ and A₁₈.) This observation shows that at least one long-lived water molecule resides within about 4 Å of each of these four DNA protons. While it is not possible to infer the number of long-lived waters from the NOE data themselves, some clues are provided by the crystal structure. Assuming that the primary spine waters are located at the base-pair steps, as in the crystal structure, each of the four adenine H2 protons is within 2.4–3.4 Å of four water protons belonging to two of the five central water molecules in the primary layer of the spine (Figure 1).⁵ In principle, the two positive cross peaks can be explained by just two long-lived water molecules (W₋₁ and W₁ in Figure 13). By symmetry, these waters must have the same residence time. On the basis of crystallographic interproton distances, the A₆ peak would then be nearly 4 times more intense than the A₅ peak. This does not appear to be the case (Figure 6), although overlap with a pure exchange peak from one of the C₁ amino protons makes it hard to quantitatively estimate the intensity of the A₅ peak. The protons of the central water molecule (W₀) are not very close to the H2 protons of A₆ and A₁₈—they would contribute only about 20% of the A₆ cross-peak intensity. It is therefore not possible to say whether the two positive cross peaks are due to 4 or 5 long-lived water molecules, although there is no reason to believe that W₀ has a shorter residence time than W₁/W₋₁ or W₂/W₋₂.

Using the interproton distances in Figure 13, we obtain for the effective two-spin separation $r_{\text{eff}} = (\sum_i r_i^{-6})^{-1/6}$ the values 2.2 Å for the A₆ cross peak (or 2.3 Å without W₀) and 2.3 Å for the A₅ cross peak. By following the zero crossing of the NOESY cross-peak intensity as a function of temperature at different magnetic field strengths, it is possible to separate τ_C and ω_D in σ_{NOE} , and hence to determine r_{eff} [see Eqs. (2) and (8)]. The only study that has pursued this approach obtained $r_{\text{eff}} = 2.6$ Å for the A₆ cross peak

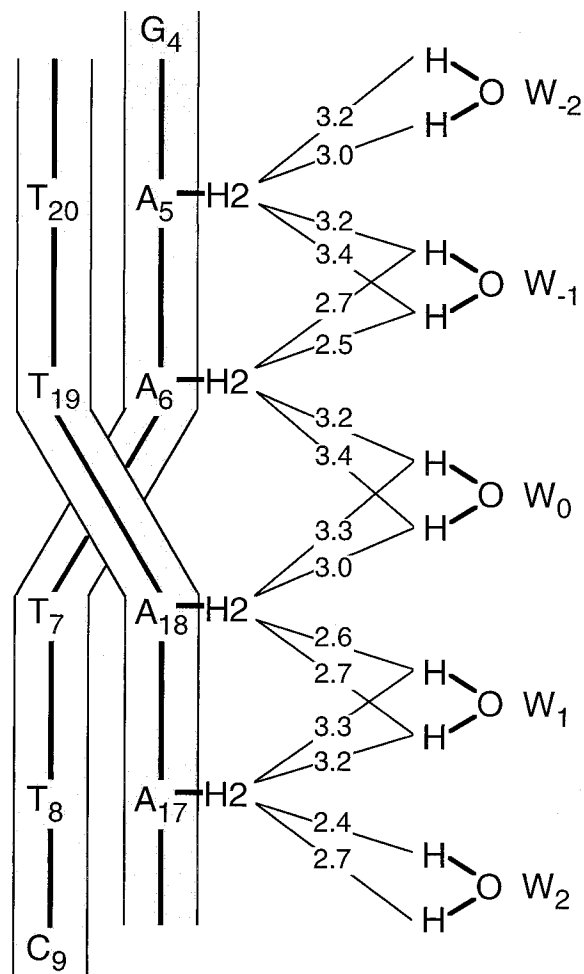


FIGURE 13 Schematic view of NOE contacts between the four adenine H2 protons and the five central water molecules in the primary layer of the spine in the minor groove of the d(CGCGAATTCGCG) duplex. These water molecules are also shown in Figure 1. The interproton distances were obtained by assuming standard covalent geometry (HOH angle, 107°) and optimal hydrogen bonds while connecting hydrogens to the heavy-atom coordinates of the 1.1 Å crystal structure (NDB code BD0007).⁵ The differences in interproton distances within the two symmetry-related (in solution) pairs of water molecules (mainly for W₂/W₋₂) may be attributed to the asymmetric crystal environment.

from the d(CGCGAATTCGCG) dodecamer.²⁰ Considering that σ_{NOE} depends on the inverse sixth power of r_{eff} , the experimental r_{eff} value yields a cross-relaxation rate that is a factor 2.7 smaller than the one calculated with crystallographically derived distances. This discrepancy might reflect differences in hydration geometry between crystal and solution. A more likely explanation, however, is that the dipolar coupling is partially averaged by internal motions. Such a

deviation from the rigid-binding limit has the effect of shifting the zero crossing of σ_{NOE} to larger values of the residence time (Figure 10), but, if the internal-motion time scale is much shorter than τ_{W} , the main effect is to multiply σ_{NOE} by a factor S^2 —the (square of the) generalized order parameter.¹⁰ (In Ref. 15, the internal motion was assumed to be in the extreme-narrowing limit, which is not necessarily the case.) To explain the σ_{NOE} discrepancy entirely by internal motions, we would thus need $S^2 = 1/2.7 = 0.37$. The ^{17}O MRD data yield $S^2 \sim 0.8$ for the d(CGCGAATTCGCG) dodecamer,¹⁶ but the order parameter for the intramolecular ^{17}O quadrupole coupling is not the same as for the intermolecular ^1H - ^1H dipole coupling.¹⁰ In particular, if the water molecules flip rapidly about the C_2 axis (as indicated by ^2H MRD data¹⁶), then $S^2(^{17}\text{O})$ is unaffected while $S^2(^1\text{H}$ - $^1\text{H})$ is reduced by a factor of about 0.8.¹⁶ Furthermore, $S^2(^1\text{H}$ - $^1\text{H})$ will be reduced by fluctuations of the interproton distance due to adenine base librations.⁴²

While the pioneering NOE studies of the d(CGCGAATTCGCG) dodecamer only reported lower bounds on τ_{W} (and these were somewhat overestimated),^{27,33} subsequent studies could determine τ_{W} quantitatively from the ratio of NOESY and ROESY cross-peak intensities^{15,16} and from the NOE zero crossing as a function of temperature as well as from off-resonance ROESY experiments.²⁰ For the A_6 cross peak, the NOESY/ROESY intensity ratio yielded $\tau_{\text{W}} = 0.6$ ns at 10°C ,¹⁵ while the zero-NOE method gave 0.5 ns at 15°C and 0.3 ns at 23°C .²⁰ (The small correction for duplex tumbling is ignored here and in the following.) These NOE results are not only mutually consistent, but also agree with the value $\tau_{\text{W}} = 0.9$ ns at 4°C obtained by the MRD method.¹⁵ Considering that the NOE and MRD methods are susceptible to quite different kinds of systematic error, this quantitative agreement is remarkable.

Most of the currently available quantitative results on residence times for water molecules in the minor groove of B-DNA duplexes are collected in Figure 14 in the form of an Arrhenius plot. Within the investigated temperature ranges, the combined zero-NOE and off-resonance ROESY data follow the Arrhenius rate law quite well. The activation enthalpy is $35\text{--}40$ kJ mol^{-1} for d(AAAAATTTT) and d(CGCGAATTCGCG) and 27 kJ mol^{-1} for d(CGCGATCGCG).²⁰ The MRD result for d(CGCGAATTCGCG) at -20°C deviates significantly from the Arrhenius fits to the NOE data obtained at higher temperatures. While the origin of this difference is unclear, it may be noted that most rate processes that require rearrangement of the hydrogen-bond network in water exhibit a distinct

curvature in an Arrhenius plot over a 50 K temperature range, particularly at subzero temperatures.

The zero-NOE data for d(CGCGAATTCGCG) in Figure 14 show a 20–40% difference in τ_{W} for the water molecules that contribute to the A_5 and A_6 cross peaks.²⁰ A similar shortening of the residence time toward the flanks of the A-tract is evident in the zero-NOE data for d(AAAAATTTT),²⁰ and in a more qualitative way, is suggested by variations in cross-peak intensities along the A-tract in other duplexes^{22,24,27,32,38} (Table II). These τ_{W} variations could be an artifact of the rigid-binding assumption.¹⁶ If the order parameter S^2 decreases towards the periphery of the A-tract, then the rigid-binding assumption would underestimate τ_{W} more for the outer adenine H2 cross peaks. But even if the τ_{W} variation is real, the most significant fact is that it is very small. Furthermore, such a narrow τ_{W} distribution would not

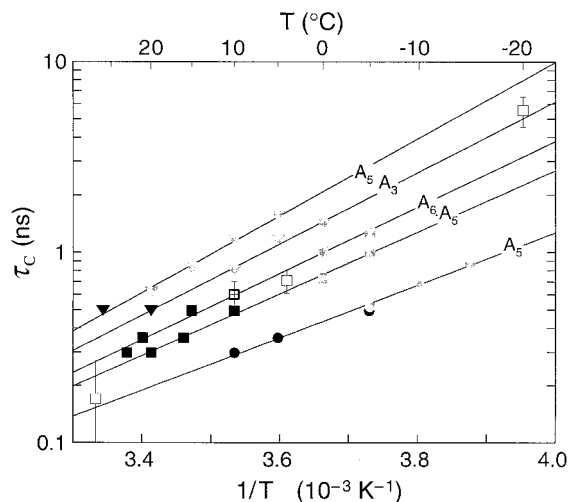


FIGURE 14 Arrhenius plot of correlation times (essentially residence times) for water molecules in the minor groove of three B-DNA duplexes: d(AAAAATTTT) (triangles), d(CGCGAATTCGCG) (squares), and d(CGCGATCGCG) (circles). Four different methods were used to obtain these results: NOE zero crossing²⁰ (solid black symbols), off-resonance ROESY²⁰ (solid gray symbols), NOESY/ROESY intensity ratio¹⁵ (open square with cross), and $^{17}\text{O}/^2\text{H}$ -MRD^{15,16} (open squares). The two sets of zero-NOE and off-resonance ROESY data for d(AAAAATTTT) and d(CGCGAATTCGCG) refer to the indicated adenine H2 cross peaks; the NOESY/ROESY datum refers to A_6 ; and the MRD data refer to all long-lived water molecules in the minor groove of d(CGCGAATTCGCG). The MRD data have been corrected to a 90:10 $\text{H}_2\text{O}:\text{D}_2\text{O}$ solvent (as used in the NOE studies), assuming that τ_{c} is proportional to the viscosity of bulk water. The solid lines resulted from linear regression to the combined zero-NOE and off-resonance ROESY data.

produce a detectable deviation from Lorentzian shape in the dispersion profiles (see previous subsection).

Since the NOE method normally can detect minor-groove water only in A-tracts, the hypothesis that τ_w correlates with groove width cannot be tested as straightforwardly as with MRD (see previous subsection). The inability to detect long-lived water molecules near CG base pairs introduces a bias in the NOE results and tends to exaggerate relative variations. Furthermore, it appears that, in the temperature range 4–10°C where most NOE studies have been carried out, many water molecules in the minor groove happen to have residence times not far from the NOE zero crossing (0.3–0.5 ns). Variations in the sign of cross-peaks can then result from rather subtle variations in water dynamics and DNA structure. The operational distinction between “long-lived” and “short-lived” water is further confounded by the variation in temperature and magnetic field between different studies.

The first indication from NOE data of a correlation between τ_w and groove width came from studies of the two dodecamers d(GTGGAATTCCAC) and d(GTGGTTAACCAC), differing only in the nucleotide sequence within the central A-tract.³⁸ The cross-peak intensities indicated longer residence times ($\tau_w > 0.3$ ns) for the AATT tract than for the TTAA tract ($\tau_w \sim 0.3$ ns), in agreement with the widely held view that a T-A step widens the groove. However, structural data (in crystal or solution) on these duplexes are not available. For the dodecamer d(CGCGTTAACGCG), which shares the six central base pairs with the TTAA dodecamer in the NOE study, the average groove width in the TTAA region is 4.4 Å, as compared to 4.2 Å in the AATT segment in d(CGCGAATTCGCG).⁵¹ While both of these A-tracts are considerably narrowed relative to canonical B-DNA (6.0 Å), the difference between them is hardly significant.

The finding in a subsequent NOE study²² of long-lived waters ($\tau_w > 0.3$ ns) near A₆ and A₇ in the decamer d(GCATTAATGC) seems to invalidate the conjecture that a T-A step disrupts the single-file hydration structure⁵⁰ and leads to short residence times.³⁸ This conjecture was also challenged by the MRD finding¹⁶ of long-lived waters in dodecamers with up to three T-A steps (see section on MRD results above). Unfortunately, no crystal structure has been reported for the decamer of the NOE study, but the structures of the closely related decamers d(CGATTAATCG)⁵² and d(CCATTAATGG)⁵³ have been determined. Whereas the latter decamer exhibits a uniformly narrow minor groove throughout the AT-TAAT region, the minor groove of the former is widest at the central T-A step, but is quite narrow at

the ends of the ATTAAT region. Since these two decamers crystallize in different space groups, the difference in groove morphology can probably be ascribed to crystal packing forces. The crystallographic data thus offer little guidance regarding groove width and hydration of d(GCATTAATGC) in solution.

The NOE study included two more decamers with a central TTAA region.²² In the nonself-complementary decamer d(GCATTAACGC) (differing by a single base pair from the previously discussed decamer), the adenine H2 cross peaks progressed from positive to negative on going from the central two AT base pairs to the outermost AT base pair (Table II). As discussed above, this could reflect an order parameter gradient. In the related decamer d(GCCTTAAAGC), there was no indication of long-lived waters at all.²² A major conclusion from this NOE study of three related decamers is that τ_w depends on nucleotide sequence in a nonlocal way—a given adenine H2 cross peak can be affected by a base-pair substitution four positions away. However, if the groove width is also a nonlocal function of nucleotide sequence, it is still possible that the residence time is governed by the local groove width. In discussing sequence effects, it should be borne in mind that, since the primary spine waters are located at the base steps, a given adenine H2 proton is engaged in NOE transfer with two water molecules that donate hydrogen bonds to four bases in three consecutive base pairs. This tends to delocalize the effect of a base-pair substitution. It should also be remembered that the difference, in terms of nanoseconds, between absence and presence of “long-lived” water may be rather small.

Rather than focusing on the variable sign of NOESY cross peaks, it may be more productive to ponder why τ_w appears to vary so little within A-tracts. The –20°C MRD study found no significant difference in residence time between the (probably nine) primary spine waters in d(CGAAAATTTTCG) and the (one or three) waters at the center of d(CGCTCTAGAGCG).¹⁶ Similarly, in the zero-NOE study, the residence times in d(AAAAATTTTT) and d(CGCGATCGCG) differed by less than a factor 5 at any temperature (and part of this difference could be an ordering effect).²⁰ For the dodecamer d(CGCAAATTTGCG) a quantitative NOESY/ROESY analysis yielded residence times in the range 0.4–1.5 ns at 10°C,²⁴ similar to the value 0.6 ns deduced for d(CGCGAATTCGCG) at the same temperature and with the same method.¹⁵ These NOE results are fully consistent with the MRD results for the same dodecamers.^{15,16}

Three NOE studies have been reported of complexes between B-DNA and drug molecules bound in the minor groove. For the complex between netropsin and d(CGCGAATTCGCG), the direct-NOE cross peaks between A₅ and A₆ and water are absent.¹⁵ This is as expected since this centrally bound drug covers nearly 6 base pairs in the minor groove and thus displaces the original spine of hydration.⁵⁴ Although a weakly positive NOESY cross peak with A₅ H2 was observed, this could be ascribed to a proton-exchange-relayed NOE with a labile amidinium proton in netropsin.¹⁵ The two water molecules at the ends of the netropsin molecule that presumably are responsible for the small ¹⁷O dispersion from the complex¹⁶ (Figure 4) would not be detected by the NOE method since they are too distant from the A₅/A₁₇ H2 protons and since CG base pairs do not provide suitable reporter protons. A somewhat different picture emerges from NOE studies of the propamidine complexes with d(CGCGAATTCGCG)³⁶ and d(CGCAAATTCGCG),²⁴ where positive NOESY cross peaks were observed between water and all adenine H2 protons (Table II). Propamidine is shorter than netropsin, covering only 4 base pairs, and the dominant binding mode is slightly asymmetric, with the drug displaced by 0.3 base pairs from the center of the A-tract.^{24,36} The primary spine waters at the base-pair steps in the GA and CAA segments may therefore survive in the complex. While some or all of these cross peaks could be proton-exchange relayed, as in the case of netropsin, it was argued that this mechanism is unimportant in the propamidine complexes.^{24,36}

Although this review focuses on the minor groove, a brief mention of major-groove hydration seems appropriate. Many NOE studies have reported water cross peaks with thymine CH₃, adenine H8, and guanine H8 protons in the major groove. The NOESY cross peaks with these protons are usually negative but are not very far from the zero crossing, and they may even become positive at lower temperatures. [The conclusion from a NOESY/ROESY study²⁴ of the d(CGCAAATTCGCG) duplex that $\tau_w = 0.5\text{--}1.5$ ns at 20°C for water molecules near G₁₀ H8 can probably be attributed to proton-exchange-relayed magnetization transfer.] The most direct information about water exchange from the major groove has been provided by a zero-NOE study, where it was concluded that $\tau_w \sim 0.4$ ns at -10°C for several duplexes.²⁰ This result suggests that the residence times of water molecules in the major groove are only an order of magnitude shorter than for the most long-lived waters in the minor groove. Is this consistent with the available MRD results?

The high-frequency plateau (α parameter) of the dispersion profile yields an average correlation time

for all water molecules coordinating the DNA duplex, including the major groove and the phosphate backbone. This average correlation time is only a factor 6 longer than for bulk water,^{15,16} whereas the residence time of long-lived minor-groove waters is 50–100 times longer than the corresponding time in bulk water (the time taken to diffuse one molecular diameter). These MRD results are not incompatible with the view that most water molecules hydrating the major groove have residence times that are merely an order of magnitude shorter than in the narrow minor groove. We note, however, that the Lorentzian spectral density in Eq. (2) may not be appropriate for analyzing NOEs from the exposed hydration sites in the major groove. Although the dipolar coupling falls off as r^{-6} , the number of water protons at a given separation increases roughly as r^2 and so does the time scale of angular modulation of the dipole coupling. The contributions to the cross-relaxation rate from different spatial regions are thus weighted as r^{-2} , and when summed up, render the cross-relaxation rate (at low frequencies) dependent on $1/b$ (with b the distance of closest approach of the two protons) rather than on $1/b^6$ (as for a single long-lived water molecule in the minor groove).^{14,41} With a more sophisticated spectral density function that takes this into account, the same NOE data would yield shorter residence times.

IONS IN THE MINOR GROOVE

By virtue of its highly charged phosphate backbone, double-helical DNA is engaged in strong electrostatic interactions. The neutralizing charge is provided by mobile counterions in the surrounding aqueous medium, and, in protein–DNA and drug–DNA complexes, also by cationic residues. With few exceptions, alkali metal counterions in nucleic acid crystals have escaped detection by x-ray diffraction. With the recent availability of atomic-resolution crystal structures of several B-DNA duplexes,³ the situation has improved. Crystallographic evidence has thus recently been presented for the partial substitution of alkali metal ions for water molecules at the floor of the minor groove in B-DNA.^{55–58}

Being isoelectronic, Na⁺ and H₂O are virtually indistinguishable by x-ray diffraction. Nevertheless, it has been argued on the basis of indirect crystallographic evidence that the primary hydration sites of the spine in the d(CGCGAATTCGCG) duplex are not exclusively occupied by water molecules but are partly substituted by Na⁺ ions.^{55,57} However, this conclusion has been challenged.^{5,59} Similarly, the in-

ference of K^+ ions at the primary hydration sites in the K^+ crystal of the same duplex⁵⁶ has been criticized.⁵⁹ Even if one agrees that there exists no crystallographic evidence for partial Na^+ or K^+ substitution for water molecules in the minor-groove spine of hydration, this does not necessarily mean that such ions are not there. X-ray crystallography simply cannot detect them. The case is more favorable for the heavier alkali metal ions. A Rb^+ ion has thus been localized (with about 50% occupancy) at the central AT step of the d(CGCGAATTCGCG) duplex.⁵⁸ As regards Cs^+ , the situation is less clear. Whereas fiber diffraction data from phage T2 CsDNA were successfully modeled with fully occupied Cs^+ sites in 6 out of 10 base stacking types,⁶⁰ a single-crystal diffraction study of the Cs^+ salt of d(CGCGAATTCGCG) ruled out Cs^+ penetration of the minor groove.⁵⁸

Even if the duplex morphology can be shown to be nearly the same in solution as in the crystal, the probability that a nominal solvation site in the minor groove is occupied by a certain type of ion may be quite different under the two conditions. In particular, the cryogenic temperatures used in all recent crystallographic work may drastically shift the enthalpy–entropy balance of ion–water substitution. The low water content and crystal packing effects are also of concern. Solution studies are therefore needed to settle the issue of sequence-specific counterion binding to DNA under physiological conditions. Molecular dynamics (MD) simulations can in principle provide this type of information. A recent MD study thus showed that a Na^+ ion resides (with >50% occupancy) at the central AT step of the d(CGCGAATTCGCG) duplex,^{61,62} a location that is known to have a uniquely low electrostatic potential.^{61,63} Another MD study found Na^+ ions (with 5–40% occupancy) at primary solvation sites throughout the minor and major grooves of the d(CGCGAATTCGCG) duplex.⁶⁴ Even Cl^- ions were found to substitute for primary hydration waters in the minor groove.⁶⁴ At present, however, MD results bearing on the issue of ion penetration of the minor groove must be viewed with caution. Depending on the force field used, duplex morphologies resembling either the A-form or the B-form are obtained.⁶⁵ Furthermore, none of the standard force fields directly incorporate polarization effects, which may be crucial for the energetics of ion–water substitution in the minor groove.

Partial ion occupancy of a few hydration sites in the minor groove would hardly be detected via the reduced hydration as seen by the MRD and NOE methods. It is necessary to directly monitor the magnetic resonance of the ion. Nuclear magnetic resonance has a long record in the study of the diffuse

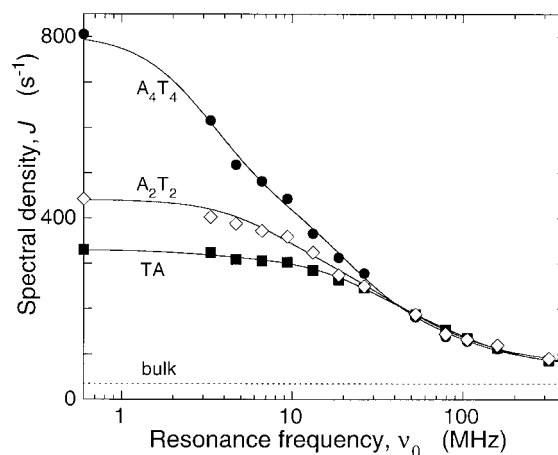


FIGURE 15 Dispersion of the ^{23}Na spectral density $J(\omega)$ from ca. 8 mM aqueous solutions of the dodecamers d(CGAAATTTTCG) (A_4T_4), d(CGCGAATTCGCG) (A_2T_2), and d(CGCTCTAGAGCG) (TA), all at 4°C and pH 7.0 (no added salt).¹¹ The points on the vertical axis represent $J(0)$. The curves represent fits to a function with three Lorentzian components plus a constant (frequency-independent) contribution.

counterion atmosphere around DNA,¹⁹ but has only recently been used to probe sequence-dependent association of monovalent ions to B-DNA oligonucleotides.^{11,13} Nuclear magnetic resonance has considerable potential in this area and more results can be expected in the near future. In the following, we summarize what has been learnt so far.

MRD Results

Among the alkali metals, ^{23}Na is best suited for nmr quadrupole relaxation studies and a large number of such studies have been carried out on DNA.¹⁹ A general conclusion from these studies is that monovalent counterion binding to DNA is loose and delocalized, without any dehydration or sequence-specific features.¹⁹ However, previous ^{23}Na nmr experiments were not optimally designed to test for sequence-specific Na^+ binding in the minor groove. Whereas most ^{23}Na relaxation studies have been restricted to one or a few frequencies (or magnetic fields), nearly two decades of frequency must be covered to unambiguously separate the static (β) and dynamic (τ_c) information. In other words, a ^{23}Na MRD study is required.

A ^{23}Na MRD study has recently been performed on the sodium salts of the dodecamers d(CGAAATTTTCG), d(CGCGAATTCGCG), and d(CGCTCTAGAGCG).¹¹ As in previous water MRD work,^{15,16} the minor-groove binding drug netropsin was used for lo-

calization, in this case, of groove-bound Na^+ ions. Because ^{23}Na relaxation is measurably biexponential, it is possible to determine the quadrupolar spectral density $j_Q(\omega)$ directly. It is therefore convenient to incorporate the effect of exchange averaging directly in the spectral density function by defining an effective spectral density $J(\omega)$ as [see Eqs. (1) and (2)]

$$J(\omega) = j_{\text{bulk}} + \alpha + \beta\tau_C/[1 + (\omega\tau_C)^2] \quad (12)$$

The β parameter is still given by Eq. (3), where N_T now denotes the total number of Na^+ ions per duplex and N_β the number of long-lived Na^+ ions. Further, the correlation time τ_C is given by Eq. (4) with τ_W replaced by the ion residence time τ_I .

Figure 15 shows the dispersion of $J(\omega)$ for the three investigated dodecamers. A pronounced dependence on nucleotide sequence is evident, where $J(\omega)$ increases with the length of the A-tract. In all cases, the shape of $J(\omega)$ is distinctly non-Lorentzian, i.e., several Lorentzian terms must be included in Eq. (12). The data for the three dodecamers converge above 50 MHz, indicating that the high-frequency components of $J(\omega)$ are due to Na^+ ions that do not interact specifically with the DNA duplex. The lowest-frequency Lorentzian component exhibits the strongest sequence dependence and thus reflects those Na^+ ions that are most intimately associated with the DNA. The correlation time τ_C of 20–40 ns for this counterion fraction agrees roughly with the DNA tumbling time, estimated to 40 ns in a separate ^{31}P relaxation experiment. In view of Eq. (4), τ_C can therefore be regarded as a lower bound for the residence time τ_I of these specifically bound Na^+ ions. However, since the $J(\omega)$ values in Figure 15 are similar to those obtained for a 146-bp DNA fragment^{66,67} (with much longer tumbling time), τ_I must be close to the observed τ_C .

To determine the location of the specifically bound Na^+ ions, the $J(\omega)$ dispersions were also determined after addition of one equivalent of netropsin.¹¹ Whereas netropsin binding reduces the magnitude of all components of $J(\omega)$, the lowest-frequency component decreases most dramatically and is virtually eliminated for d(CGCGAATTCGCG). It can therefore be concluded that the specifically bound Na^+ ions reside in the minor groove. For d(CGCGAATTCGCG), netropsin is known to bind in the central A-tract,⁵⁴ where the minor groove is most strongly narrowed. This region must therefore also contain the strongest Na^+ binding site(s). The larger low-frequency dispersion for d(CGAAAATTTTCG) (Figure 15) and its less complete elimination by netropsin are consistent with the longer narrowed A-tract (nearly

twice the length of the netropsin molecule) in this dodecamer. The d(CGCTCTAGAGCG) duplex has a uniformly wide minor groove in the crystal⁴⁴ and the relatively small low-frequency dispersion (Figure 15) therefore suggests that the affinity of Na^+ binding is reduced by a wide groove. Nevertheless, the observation of a significant low-frequency component also for this dodecamer shows that an AT step is not necessary for long-lived Na^+ binding. The incomplete elimination of the low-frequency component by netropsin may reflect a weaker (or asymmetric) binding of the drug to the this duplex.

The number N_β of long-lived Na^+ ions in the minor groove can be obtained from the magnitude (β) of the low-frequency dispersion step via Eq. (3). The quadrupole frequency ω_Q for a Na^+ ion at one of the primary hydration sites in the minor groove can be estimated from the partial charges of nearby DNA and water atoms or from ^{23}Na nmr studies of Na^+ ions with similar coordination geometry. Very similar results are obtained by the two methods. In this way, N_β values of 0.01 for d(CGCTCTAGAGCG) and 0.05 for the other two dodecamers were obtained at a total Na^+ concentration of 0.4M.¹¹ If Na^+ ions bind to a single site, the occupancy is therefore merely a few percent and the binding constant is about 0.1M^{-1} for the dodecamers with the longer A-tracts. The low occupancy implies that Na^+ binding in the minor groove is a rare event—on average, the site is occupied by a Na^+ ion for 50 ns, say, and is then visited by some 1000 water molecules, each one residing on average 1 ns,^{15,20} before another ion enters the site. Such infrequent intrusions of Na^+ into the minor groove are not likely to be sampled even in a 10 ns MD trajectory, nor would such low occupancies be detectable by x-ray diffraction. (However, the ion occupancy might be larger at cryogenic temperatures.) Furthermore, with an occupancy of only a few percent, groove-bound ions are not likely to contribute importantly to the ensemble of DNA structures present under physiological conditions. In particular, groove-bound Na^+ ions do not appear to play a major role in A-tract bending or groove narrowing.^{55,57,61,62}

The relative affinities of different monovalent counterions for the specific binding site(s) in the minor groove of d(CGCGAATTCGCG) were assessed by single-frequency ^{23}Na relaxation measurements as a function of the concentration added KCl, RbCl, CsCl, or NH_4Cl .¹¹ The results of these competition experiments indicate that K^+ , Rb^+ , and Cs^+ all bind with similar or slightly higher affinity than Na^+ , while NH_4^+ binding is an order of magnitude stronger. These relative affinities agree qualitatively with re-

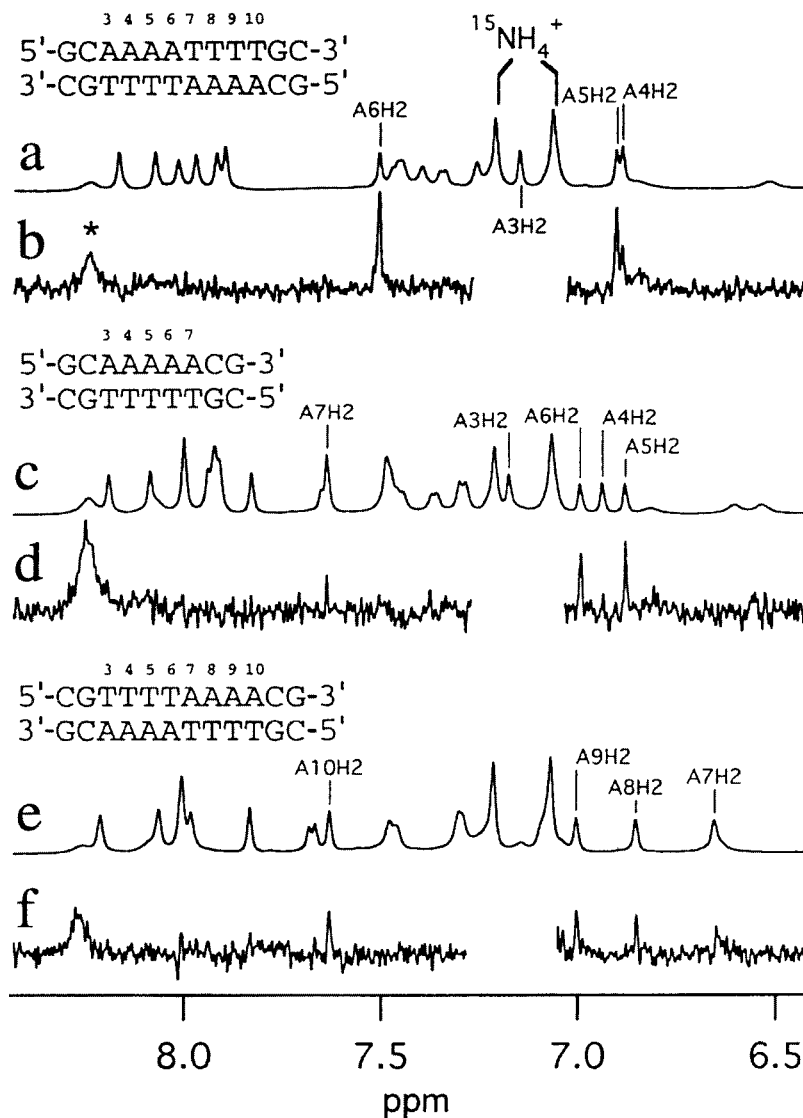


FIGURE 16 One-dimensional ^1H NOESY spectra, with selective excitation at the frequency of the $^{15}\text{NH}_4^+$ protons, recorded at 0°C from 2–3.5 mM aqueous solutions (5% D_2O) of the three indicated B-DNA duplexes at pH 5.0.¹³ The samples contained 4 mM $^{15}\text{NH}_4^+$ and 60 mM Li^+ . For each duplex, the upper trace (a,c,e) is a normal NOESY spectrum, whereas the lower trace (b,d,f) is a ^{15}N -filtered NOESY spectrum where only the magnetization transferred via ^{15}N is detected. Since the signal was acquired without ^{15}N decoupling, the ^1H resonance of $^{15}\text{NH}_4^+$ is split into a doublet. (Reprinted from *Journal of Molecular Biology*, 286, Hud, N. V., Sklenar, V., Feigon, J., “Location of Ammonium,” p. 654, copyright 1999, by permission of the publisher Academic Press.)

sults from previous ^{23}Na nmr studies of competitive counterion binding to polymeric DNA.⁶⁸

NOE Results

The NOE method cannot directly monitor the binding of alkali metal ions to DNA since these nuclei do not provide the required sensitivity and resolution. However, the ammonium ion contains four protons

and can be used for NOE studies in much the same way as water. Although the electron distribution and coordination preferences of NH_4^+ are not the same as for spherically symmetric monatomic ions, the size of the NH_4^+ ion matches H_2O and is close to K^+ and Rb^+ . In bulk aqueous solution, the ammonium protons exchange with water protons through the OH^- catalyzed mechanism so that the lifetime of the NH_4^+ protons is in the millisecond range at pH 7 (as com-

monly used for DNA studies) and room temperature.⁶⁹ Even at 10°C, the ^1H resonance from NH_4^+ in bulk solution at pH 7 is exchange-broadened beyond detection.⁷⁰ To slow down the proton exchange, NOE studies of NH_4^+ binding to DNA duplexes have been conducted at pH 5 and 0°C.¹³

We discuss now the recent NOE study of NH_4^+ binding to the B-DNA dodecamers d(GCAAATTTTGC), d(CGTTTTAAACG), and d(GCAAACGTTTGC), and to the nonamer d(GCAAAAACG).¹³ In a 2D-NOESY spectrum (acquired with ^{15}N decoupling) of d(GCAAATTTTGC) at 0°C and pH 5 and a 1:2:25 concentration ratio of duplex: $^{15}\text{NH}_4^+:\text{Na}^+$, positive cross peaks were observed between water and the H2 protons of A_4 , A_5 , and A_6 , and between $^{15}\text{NH}_4^+$ and the H2 protons of A_5 and A_6 . An intense pure exchange peak was also observed between $^{15}\text{NH}_4^+$ and water, raising the possibility that the $^{15}\text{NH}_4^+$ cross peaks with H2 protons are produced by the proton-exchange-relayed pathway $(^{15}\text{NH}_4^+)_{\text{bulk}} \rightarrow (\text{H}_2\text{O})_{\text{bulk}} \rightarrow (\text{H}_2\text{O})_{\text{groove}} \rightarrow (\text{A}_n \text{H2})$ rather than by NOE transfer from groove-bound ammonium ions via the direct pathway $(^{15}\text{NH}_4^+)_{\text{bulk}} \rightarrow (^{15}\text{NH}_4^+)_{\text{groove}} \rightarrow (\text{A}_n \text{H2})$. To exclude this possibility, the 2D-NOESY spectrum was also recorded with irradiation of the water resonance during the mixing time²¹ (see subsection NOE Spectroscopy above). In this spectrum, the water-H2 cross peaks were absent, whereas the $^{15}\text{NH}_4^+$ -H2 cross peaks had undiminished intensity. This indicates that NH_4^+ ions do indeed penetrate to the floor of the minor groove with a residence time $\tau_1 > 0.3$ ns at 0°C. Due to spectral overlap, any cross peaks with the H2 protons of A_3 and A_4 could not be detected. However, cross peaks were observed (also with water irradiation) between $^{15}\text{NH}_4^+$ and the deoxyribose H4' protons (which line the minor groove) of several adenines and thymines, including T_{10} , but not with any cytosine or guanine H4' protons. This indicates that NH_4^+ ions can bind to all primary solvation sites within the A-tract. No $^{15}\text{NH}_4^+$ cross peaks were observed with protons in a major groove.

Figure 16 shows one-dimensional ^1H NOESY spectra, recorded with and without ^{15}N filtering, for three duplexes. For d(GCAAATTTTGC), cross peaks of comparable intensity are now visible with the H2 protons of all four adenines. In the ^{15}N -filtered spectrum, the A_6 peak is most intense, suggesting that the central A-T step is the preferred location for NH_4^+ . However, in the d(CGTTTTAAACG) duplex, cross peaks are also observed with the H2 protons of all adenines, including A_7 at the T-A step (Figure 16). In contrast, no significant cross peaks were observed for the dodecamer d(GCAAACGTTTGC), suggesting that NH_4^+ binds only to A-tracts

extending over at least four base pairs. Finally, for the nonself-complementary nonamer d(GCAAAAACG), cross peaks of comparable intensity were observed with the H2 protons of all five adenines (Figure 16).

On the basis of these results, it was argued that NH_4^+ binds preferentially to narrow regions of the minor groove. While the absence of cross peaks with the H4' protons in the CG regions of d(GCAAAATTTTGC) does indicate a preference for AT base pairs, the relative binding affinities at different sites within A-tracts are more difficult to establish. The variation in cross-peak intensity is not dramatic and could be due to different binding geometry rather than different occupancy. Furthermore, the current picture of sequence-dependent groove width variation is not clear-cut. Although the NOE data do not provide the ion occupancy, the observation of (more intense) water cross peaks with the same H2 protons shows that the ion occupancy can only be partial. For the d(CGCGAATTCGCG) duplex, ^{23}Na MRD competition experiments¹¹ indicated a NH_4^+ binding constant of less than $2M^{-1}$ (at 4°C), whereas a much larger binding constant ($20\text{--}30M^{-1}$) would be required to achieve even 10% NH_4^+ occupancy under the conditions of the NOE study (with 10–15-fold excess of Na^+ or Li^+ ions). It seems unlikely that the NOE method could detect an ion occupancy much lower than 10%.

This work was supported by the Crafoord Foundation, the Royal Academy of Sciences, and the Swedish Natural Science Research Council.

REFERENCES

- Westhof, E. *Annu Rev Biophys Biophys Chem* 1988, 17, 125–144.
- Sharp, K. A.; Honig, B. *Curr Opin Struct Biol* 1995, 5, 323–328.
- Egli, M. et al., in this issue, pp. 234–252.
- Drew, H. R.; Dickerson, R. E. *J Mol Biol* 1981, 151, 535–556.
- Tereshko, V.; Minasov, G.; Egli, M. *J Am Chem Soc* 1999, 121, 470–471.
- Breslauer, K. J.; Remeta, D. P.; Chou, W.-Y.; Ferrante, R.; Curry, J.; Zaunczkowski, D.; Snyder, J. G.; Marky, L. A. *Proc Natl Acad Sci USA* 1987, 84, 8922–8926.
- Dunitz, J. D. *Chem Biol* 1995, 2, 709–712.
- Jacobson, B.; Anderson, W. A.; Arnold, J. T. *Nature* 1954, 173, 772–773.
- Reuben, J.; Shporer, M.; Gabbay, E. J. *Proc Natl Acad Sci USA* 1975, 72, 245–247.
- Halle, B.; Denisov, V. P.; Venu, K. In *Biological Magnetic Resonance*; Krishna, N. R., Berliner, L. J., Eds.; Kluwer Academic/Plenum: New York, 1999; Vol 17, chap 10.
- Denisov, V. P.; Halle, B. *Proc Natl Acad Sci USA*, in press.

12. Otting, G. In *Biological Magnetic Resonance*; Krishna, N. R., Berliner, L. J., Eds.; Kluwer Academic/Plenum: New York, 1999; Vol 17chap 11.
13. Hud, N. V.; Sklenar, V.; Feigon, J. *J Mol Biol* 1999, 286, 651–660.
14. Abragam, A. *The Principles of Nuclear Magnetism*; Clarendon Press: Oxford, 1961; chap 8.
15. Denisov, V. P.; Carlström, G.; Venu, K.; Halle, B. *J Mol Biol* 1997, 268, 118–136.
16. Jóhannesson, H.; Halle, B. *J Am Chem Soc* 1998, 120, 6859–6870.
17. Tirado, M. M.; Garcia de la Torre, J. *J Chem Phys* 1980, 73, 1986–1993.
18. Furó, I.; Halle, B. *Phys Rev E* 1995, 51, 466–477.
19. Braunlin, W. H. *Adv Biophys Chem* 1995, 15, 89–139.
20. Phan, A. T.; Leroy, J.-L.; Guéron, M. *J Mol Biol* 1999, 286, 505–519.
21. Masefski, W.; Redfield, A. G. *J Magn Reson* 1988, 78, 150–155.
22. Jacobson, A.; Leupin, W.; Liepinsh, E.; Otting, G. *Nucleic Acids Res* 1996, 24, 2911–2918.
23. Macura, S.; Ernst, R. R. *Mol Phys* 1980, 41, 95–117.
24. Lane, A. N.; Jenkins, T. C.; Frenkiel, T. A. *Biochim Biophys Acta* 1997, 1350, 205–220.
25. Griesinger, C.; Ernst, R. R. *J Magn Reson* 1987, 75, 261–271.
26. Desvaux, H.; Berthault, P.; Birlirakis, N.; Goldman, M. *J Magn Reson A* 1994, 108, 219–229.
27. Liepinsh, E.; Otting, G.; Wüthrich, K. *Nucleic Acids Res* 1992, 20, 6549–6553.
28. Hud, N. V.; Schultze, P.; Feigon, J. *J Am Chem Soc* 1998, 120, 6403–6404.
29. Leroy, J.-L.; Charretier, E.; Kochoyan, M.; Guéron, M. *Biochemistry* 1988, 27, 8894–8898.
30. Maltseva, T. V.; Agback, P.; Chattopadhyaya, J. *Nucleic Acids Res* 1993, 21, 4246–4252.
31. Maltseva, T. V.; Roselt, P.; Chattopadhyaya, J. *Nucleosides Nucleotides* 1998, 17, 1617–1634.
32. Fawthrop, S. A.; Yang, J.-C.; Fisher, J. *Nucleic Acid Res.* 1993, 21, 4860–4866.
33. Kubinec, M. G.; Wemmer, D. E. *J Am Chem Soc* 1992, 114, 8739–8740.
34. Kubinec, M. G.; Culf, A. S.; Cho, H.; Lee, D. C.; Burkham, J.; Morimoto, H.; Williams, P. G.; Wemmer, D. E. *J Biomol NMR* 1996, 7, 236–246.
35. Zhou, D.; Bryant, R. G. *J Biomol NMR* 1996, 8, 77–86.
36. Jenkins, T. C.; Lane, A. N. *Biochim Biophys Acta* 1997, 1350, 189–204.
37. Maltseva, T. V.; Altmann, K.-H.; Egli, M.; Chattopadhyaya, J. *J Biomol Struct Dynam* 1998, 16, 569–578.
38. Liepinsh, E.; Leupin, W.; Otting, G. *Nucleic Acids Res* 1994, 22, 2249–2254.
39. Leporc, S.; Mauffret, O.; El Antri, S.; Convert, O.; Lescot, E.; Tevanian, G.; Fermandjian, D. *J Biomol Struct Dynam* 1998, 16, 639–649.
40. Sunnerhagen, M.; Denisov, V. P.; Venu, K.; Bonvin, A. M. J. J.; Carey, J.; Halle, B.; Otting, G. *J Mol Biol* 1998, 282, 847–858.
41. Halle, B. In *Hydration Processes in Biology: Theoretical and Experimental Approaches*; Bellissent-Funel, M.-C., Ed.; IOS Press: Amsterdam, 1999.
42. Robinson, B. H.; Drobny, G. P. *Methods Enzymol* 1995, 261, 451–509.
43. Denisov, V. P.; Venu, K.; Peters, J.; Hörlein, H. D.; Halle, B. *J Phys Chem B* 1997, 101, 9380–9389.
44. Urpi, L.; Tereshko, V.; Malinina, L.; Huynh-Dinh, T.; Subirana, J. A. *Nature Struct Biol* 1996, 3, 325–328.
45. Edwards, K. J.; Brown, D. G.; Spink, N.; Skelly, J. V.; Neidle, S. *J Mol Biol* 1992, 226, 1161–1173.
46. Nelson, H. C. M.; Finch, J. T.; Luisi, B. F.; Klug, A. *Nature* 1987, 330, 221–226.
47. DiGabriele, A. D.; Steitz, T. A. *J Mol Biol* 1993, 231, 1024–1039.
48. Burkhoff, A. M.; Tullius, T. D. *Nature* 1988, 331, 455–457.
49. Hagerman, P. J. *Nature* 1986, 321, 449–450.
50. Chuprina, V. P. *Nucleic Acids Res* 1987, 15, 293–311.
51. Balendiran, K.; Rao, S. T.; Sekharudu, C. Y.; Zon, G.; Sundaralingam, M. *Acta Cryst D* 1995, 51, 190–198.
52. Quintana, J. R.; Grzeskowiak, K.; Yanagi, K.; Dickerson, R. E. *J Mol Biol* 1992, 225, 379–395.
53. Goodsell, D. S.; Kaczor-Grzeskowiak, M.; Dickerson, R. E. *J Mol Biol* 1994, 239, 79–96.
54. Goodsell, D. S.; Kopka, M. L.; Dickerson, R. E. *Biochemistry* 1995, 34, 4983–4993.
55. Shui, X.; McFail-Isom, L.; Hu, G. G.; Williams, L. D. *Biochemistry* 1998, 37, 8341–8355.
56. Shui, X.; Sines, C. C.; McFail-Isom, L.; VanDerveer, D.; Williams, L. D. *Biochemistry* 1998, 37, 16877–16887.
57. McFail-Isom, L.; Sines, C. S.; Williams, L. D. *Curr Opin Struct Biol* 1999, 9, 298–304.
58. Tereshko, V.; Minasov, G.; Egli, M. *J Am Chem Soc* 1999, 121, 3590–3595.
59. Chiu, T. K.; Kaczor-Grzeskowiak, M.; Dickerson, R. E. *J Mol Biol* 1999, 292, 589–608.
60. Bartenev, V. N.; Golovamov, E. I.; Kapitonova, K. A.; Mokulskii, M. A.; Volkova, L. I.; Skuratovskii, I. Ya. *J Mol Biol* 1983, 169, 217–234.
61. Young, M. A.; Jayaram, B.; & Beveridge, D. L. *J Am Chem Soc* 1997, 119, 59–69.
62. Young, M. A.; Ravishanker, G.; Beveridge, D. L. *Biophys J* 1997, 73, 2313–2336.
63. Lavery, R.; Pullman, B. *J Biomol Struct Dynam* 1985, 5, 1021–1032.
64. Feig, M.; Pettitt, B. M. *Biophys J* 1999, 77, 1769–1781.
65. Pettitt, B. M. In this issue.
66. van Dijk, L.; Gruwel, M. L. H.; Jesse, W.; de Bleijser, J.; Leyte, J. C. *Biopolymers* 1987, 26, 261–284.
67. Groot, L. C. A.; van der Maarel, J. R. C.; Leyte, J. C. J. *Phys Chem* 1994, 98, 2699–2705.
68. Bleam, M. L.; Anderson, C. F.; Record, M. T. *Proc Natl Acad Sci USA* 1980, 77, 3085–3089.
69. Eigen, M. *Angew Chemie Int Ed* 1964, 3, 1–72.
70. Hud, N. V.; Schultze, P.; Sklenar, V.; Feigon, J. *J Mol Biol* 1999, 285, 233–243.